

OVERPRESSURED MARINE SEDIMENTS:
THE THERMOMECHANICS OF PROGRESSIVE BURIAL

Final Report for Phase II
for
U. S. Department of Interior
U. S. Geological Survey
U. S. G. S. Grant No. 14-08-0001-G-444

A report from the
Texas A&M Research Foundation
College Station, Texas
Project No. 3641

by

Louis J. Thompson
Civil Engineering Department
Texas A&M University
College Station, Texas
77843

July 24, 1979

This work was sponsored by the
U. S. G. S. as a part of the Research
Program in OSC Oil and Operations
Conservation Division
12201 Sunrise Valley Drive
Reston, Va. 22092
John Gregory - Program Manager



Equilibrium and experimental test results show that the variation in pore water pressure with respect to depth in a constant porosity formation must be equal to a constant that depends on the specific gravity of the mineral and the porosity of the formation.

As the type of mineral changes in a formation these constants change. The compressibility coefficients of a formation can be related to the Atterberg limits of the formation minerals. The total overburden stress can be computed from the porosity measurement on the cuttings and the compressibility constants estimated from the Atterberg limit tests on the cuttings. The pore pressure in the shale can be calculated from equilibrium conditions. The pore water pressure in the sands must be less than the pore water pressure in the shale. These calculations can be programmed on a mini-calculator for ease of operation of field personnel so that expected pore pressure can be estimated before the formation is penetrated and while drilling progresses.

Using equilibrium, conservation of mass, and the experimental results, the governing partial differential equation for porosity as a function of depth and time has been derived. It has a unique solution.

Using the energy equation and experimental results for the recoverable strain energy and the heat conductivity, another governing partial differential equation has been derived for the temperature and porosity as a function of depth and time. Further decoupling of the governing differential equations should make it possible to predict the porosity and temperature as a function of depth and time.

The coefficient of lateral earth stress at rest and the hydrofracture pressure are also related to the porosity and Atterberg limits. Hydrofracture could not happen if the fluid pressure was neutral as postulated by the effective stress principle.

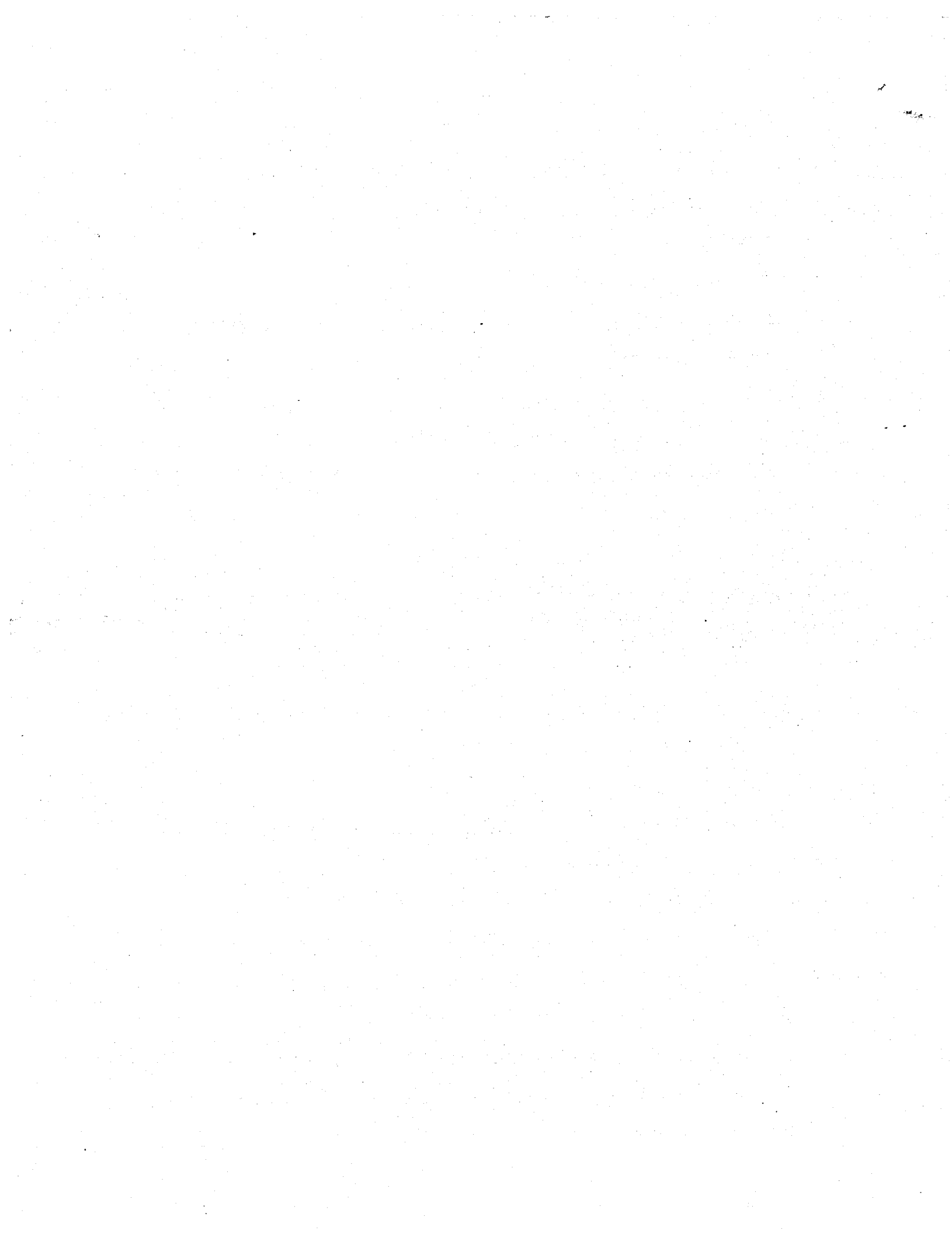


TABLE OF CONTENTS

	Page
ABSTRACT	i
TABLE OF CONTENTS	iii
LIST OF FIGURES	v
LIST OF TABLES	vii
ACKNOWLEDGMENTS	viii
1. OBJECTIVE OF RESEARCH	1
2. INTRODUCTION	2
3. EQUILIBRIUM AND THE EFFECTIVE FORCE CONCEPT	6
4. EXPERIMENTAL WORK - COMPRESSIBILITY, PERMEABILITY AND HEAT CONDUCTIVITY	75
5. EXPERIMENTAL RESULTS	23
Compressibility	23
Unloading	27
Rate of Change of Strain Energy	30
Cohesion	31
Pore Pressures	32
Permeability	34
Thermal Conductivity and Specific Heat of Sediment	34
6. CONSERVATION OF MASS AND DARCY'S LAW - DERIVATION OF THE PROGRESSIVE BURIAL CONSOLIDATION EQUATION	41
7. HYDROSTATIC PRESSURE - DEPTH RELATIONSHIP FOR INTERSTITIAL SALT WATER	46
8. POROSITY-DEPTH RELATIONSHIP FOR NORMALLY CONSOLIDATED FORMATIONS AT CONSTANT TEMPERATURES	58

TABLE OF CONTENTS (CONT'D)

	Page
9. VARIATION IN PORE WATER PRESSURE IN CONSTANT POROSITY FORMATIONS	65
10. EQUILIBRIUM REQUIREMENT FOR PORE WATER PRESSURE AT INTERFACES	70
11. THERMODYNAMICS OF PROGRESSIVE BURIAL OF SEDIMENT	74
12. A PRACTICAL APPLICATION OF RESEARCH; ESTIMATION OF PORE WATER PRESSURE WHILE DRILLING	85
13. CONCLUSIONS AND RECOMMENDATIONS	88
14. REFERENCES	92



LIST OF FIGURES

Figure		Page
1	GENERALIZED RELATIONS BETWEEN DEPTH AND VARIOUS PROPERTIES FOR OVERPRESSURED CLASTIC ROCKS	3
2.	SHALE, SAND AND WATER FORCES AS A FUNCTION OF DEPTH . .	7
3.	MECHANISTIC ANALOGY FOR FORCES IN SEDIMENT AND WATER .	8
4.	POWER LAW REPRESENTATION OF THE RATIO OF THE AREA OF THE WATER AND AREA OF THE MINERAL TO THE TOTAL AREA AS A FUNCTION OF POROSITY RATIO	10
5.	HIGH PRESSURE STAINLESS STEEL CONSOLIDOMETER	16
6.	LEVER LOADING SYSTEM AND CONSOLIDOMETER	17
7.	SCHEMATIC OF HIGH PRESSURE STAINLESS STEEL CONSOLIDOMETER	18
8.	SCHEMATIC OF CONSOLIDOMETER AND ITS MEASURING SYSTEM	19
9.	HEAT CONDUCTIVITY TRANSDUCER AND RECORDING EQUIPMENT .	21
10.	PLOT OF CONSOLIDATION STRESS AS A FUNCTION OF POROSITY RATIO (LABORATORY TEST RESULTS)	25
11.	TYPICAL LOADING AND UNLOADING FUNCTION FOR MARINE SEDIMENT IN UNIAXIAL COMPRESSION	28
12.	PLOT OF SALT WATER PERMEABILITY AS A FUNCTION OF POROSITY RATIO (LABORATORY TEST RESULTS)	35
13.	THERMAL CONDUCTIVITY VERSUS POROSITY RATIO FROM THE LITERATURE	36
14.	LABORATORY THERMAL CONDUCTIVITY FOR KAOLINITE MEASURED DURING CONSOLIDATION	37

Figure		Page
15	BOTTOM-HOLE TEMPERATURE FOR SOME WELLS, CHOCOLATE BAYOU FIELD, BRAZORIA COUNTY, TEXAS	47
16	BOTTOM-HOLE PORE PRESSURE FOR SOME WELLS, CHOCOLATE BAYOU FIELD, BRAZORIA COUNTY, TEXAS	48
17	ISOTHERMAL GRADIENT MAP	49
18	DEVIATION OF CALCULATED HYDROSTATIC PRESSURE CALCULATED BY TAKING INTO CONSIDERATION THE EFFECT OF THE THERMAL GRADIENT AND HYDROSTATIC PRESSURE CALCULATED BY ASSUMING THE SPECIFIC GRAVITY OF WATER IS ONE	56
19	SPECIFIC GRAVITY OF SEA WATER HYDROSTATICALLY COMPRESSED WITH DIFFERENT THERMAL GRADIENTS	57
20	PLOT OF COMPUTED POROSITY RATIO DEPTH RELATION- SHIP WITH HYDROSTATIC PORE STRESS AT CONSTANT TEMPERATURE	62
21	CHANGE IN PRESSURE-DEPTH RATIO IN CONSTANT POROSITY FORMATION	66
22	CONTOUR MAP OF HEAT FLOW	76

ACKNOWLEDGEMENTS

The research was sponsored by the U. S. Geological Survey as part of the Research Program in OSC Oil and Gas Operations, Grant No. 14-08-0001-G-444.

The unstinting aid and support rendered by John Gregory, U. S. Geological Survey, Research Program Manager is thoroughly appreciated. William Sweet, Oceanographer, U. S. G. S. Conservation Division, Gulf of Mexico Region, Metairie, Louisiana was the technical monitor for the project. His advice and counsel is gratefully acknowledged. Dave Powley, Senior Scientist, Amoco Research Labs, Tulsa, Oklahoma came to Texas A&M University and lectured for 2 days to present the industrial state-of-the-art for dealing with deeply buried overpressured rock formations. He read the complete report, pointed out errors and made many constructive suggestions. Amoco is thanked for allowing Dave Powley to provide field data and for his unstinting help.

William McGuire, Professor of Petroleum Engineering and Douglas Von Gonten, Head of Petroleum Engineering, Texas A&M University, helped to pose the problem and both have helped and given advice on the project. This effort is acknowledged and appreciated.

William Bryant, Marine Geology-Oceanography Department, Texas A&M University, furnished samples to be tested and provided all geological



1. OBJECTIVE OF RESEARCH

The long term purpose of this study is to develop a consolidation of the sediment theory applicable to the progressive burial of ocean bottom sediments which will give the porosity of the sediment as a function of depth and time for various rates of deposition on the ocean bottom. It is hoped that the theory will explain how geological formations develop and how their contained fluids derive their energy. It is also hoped that the theory will explain how pore water pressure at both great and shallow depths can exceed either the hydrostatic or geostatic pressure and how when these overpressured formations are penetrated they can release sufficient quantities of energy to cause blowouts of catastrophic proportions.

2. INTRODUCTION

Blowouts are one of the major causes of failure of offshore wells. Great loss of lives and property result and the ocean is substantially polluted with many of the accidents. Overpressured formations may also be one of the causes of ocean bottom oil seeps. Beneficially, it is generally believed that overpressured formations provide the major energy source (drives) for artesian production of oil, gas and fresh water (24). However there is no common agreement concerning the source of energy that causes overpressures to develop.

Overpressures are quite prevalent in both shallow clays and deep rock formations, both generally in regions where the rate of deposition is rapid. Overpressured shallow clays usually have low to very low strength and may be the major cause of submarine slope instabilities and of the low bearing strength for ocean bottom founded structures. Overpressured deep rock formations generally have considerable strength, however. Figure 1 represents the generalized relations between depth and pore pressure, temperature, porosity, electrical resistivity and some velocity. The various profiles are for the Gulf coast region extending from New Orleans, Louisiana to Brownsville, Texas.

Subsidence may result when the pore pressure is lowered in a sand formation. Large hydraulic gradients may be established in the higher pressured adjacent clays causing drainage into the sands. The clay, being compressible, densifies with drainage whereas the sand, being nearly incompressible, does not.

Formations may have pore pressures that are subnormal, normal or abnormal. Normal pore pressure is usually thought of as the hydrostatic water pressure. If the water stress exceeds the geostatic or overburden stress the pore fluid stress may be said to be hypergeostatic. Both

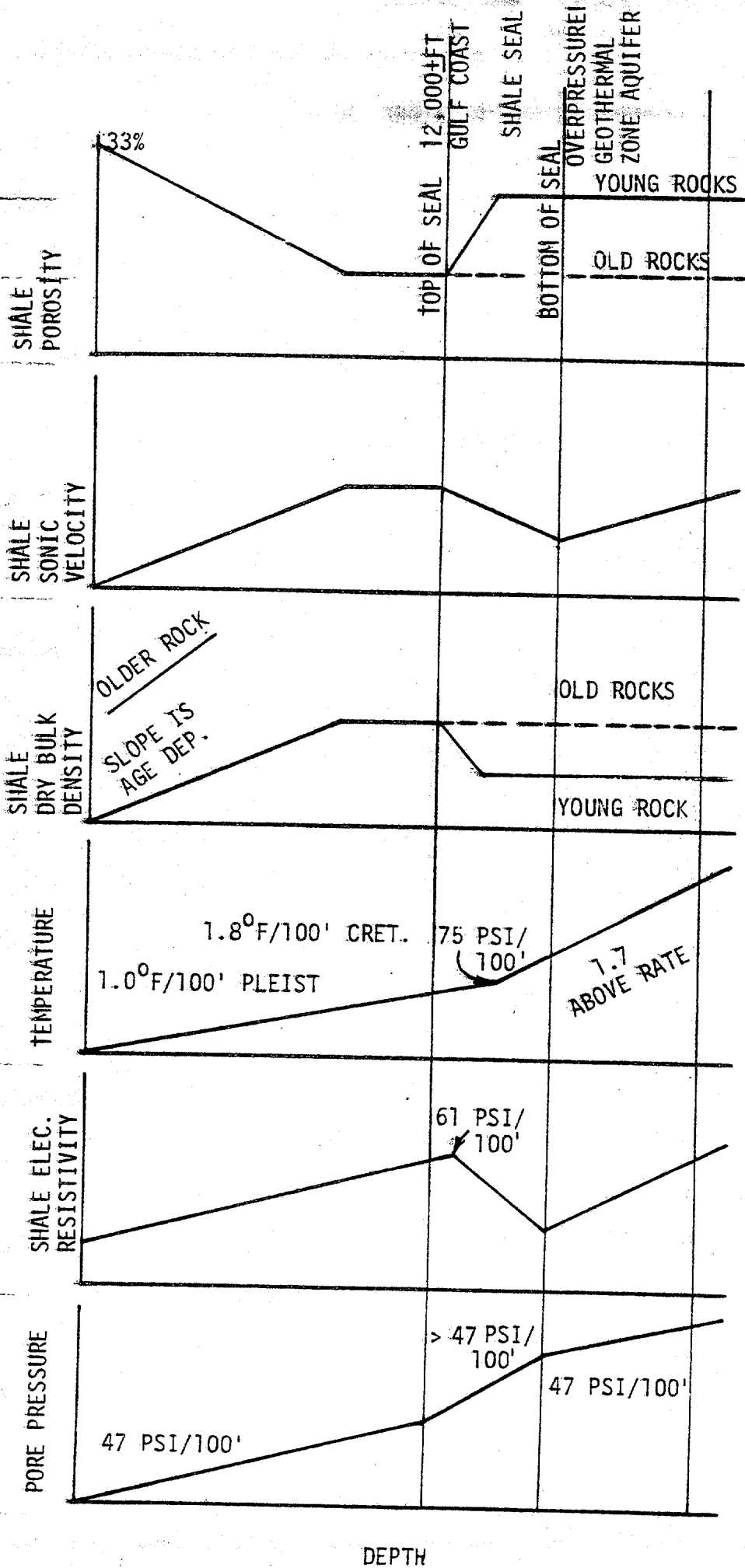


FIG. 1

GENERALIZED RELATIONS BETWEEN DEPTH AND
VARIOUS PROPERTIES FOR OVERPRESSURED CLASTIC ROCKS

abnormal and hypergeostatic formations are sometimes termed overpressured.

When a well is drilled into a porous formation and its pore fluid pressure is greater than the drilling fluid pressure at the same depth, the formation fluid may flow into the well bore diluting the drilling fluid and as the formation fluid rises in the well bore dissolved gases may pop out of solution and expand due to the reduced pressure. This further reduces the specific gravity of the drilling fluid and further lowers the drilling fluid pressure which permits even higher formation flow rates into the well bore. If the well is not quickly shut in by closing the blowout preventers a catastrophic blowout may occur.

After the blowout preventers are closed the diluted well bore fluid must be circulated out and new higher density drilling fluids introduced into the well so that the drilling fluid pressure safely exceeds the formation pore pressure. However, the drilling fluid should be heavy enough for safe withdrawal of the drill pipe, but not so heavy as to unduly retard the drilling rate or to cause the formation to fracture with a circulation loss.

Blowouts occur only in porous formations that have high permeability. The shales or clays that lie above or below high pressured sands may have an even higher pore fluid pressure but their permeability is so low that they pose no threat.

The most immediate application of this partially completed research may be in making better estimations of the drilling mud weights needed to prevent a blowout from a sand member interbedded in an overpressured shale formation before drilling into the sand. If the high pressured shale formations can be recognized before the interbedded sand formations are penetrated it will be possible to save many lives and expensive property

and prevent much contamination of the ocean. An outline of such a scheme is presented in the section Possible Application of Research to Well Drilling.

3. EQUILIBRIUM AND THE EFFECTIVE FORCE CONCEPT

Terzaghi's effective stress concept is based on a theoretical condition of vanishingly small contact areas at grain to grain interfaces. Inasmuch as vanishingly small contact areas are not present in real rocks it has been recognized for years that Terzaghi's effective stress concept does not strictly apply to real rocks (30). Engineers have used it knowing that it is a partial pressure concept similar to the artifice used to study mixtures of gases (20). It is a reasonably good approximation for coarse soils and perhaps for fine grained soils that have very high porosities. However, there is some doubt that it can even be strictly applied to fine grained soils with very high porosities such as slurries that behave as heavy liquids.

Equilibrium requires that at any depth the force in the water plus the force in the sediment in any direction must be equal to the total force in that same direction. The force in the water is the water stress times the water area. The force in sediment is the sediment stress times the sediment area. The total force is the total stress times the total area. The total area is the sum of area of the water plus the area of the sediment. The total force and the water stress must be continuous functions of depth. The total force and the total stress continuously increase with depth. The stress in the sediment, the area of the sediment and the area of the water may vary erratically as long as they are piecewise continuous.

Figure 2 shows how the force in the water and the force in the mineral can change with depth going from shale into sand.

Figure 3 shows a mechanistic analogy for soil or rock. The top diagram shows the compression in the mineral grains is represented by σ' acting over

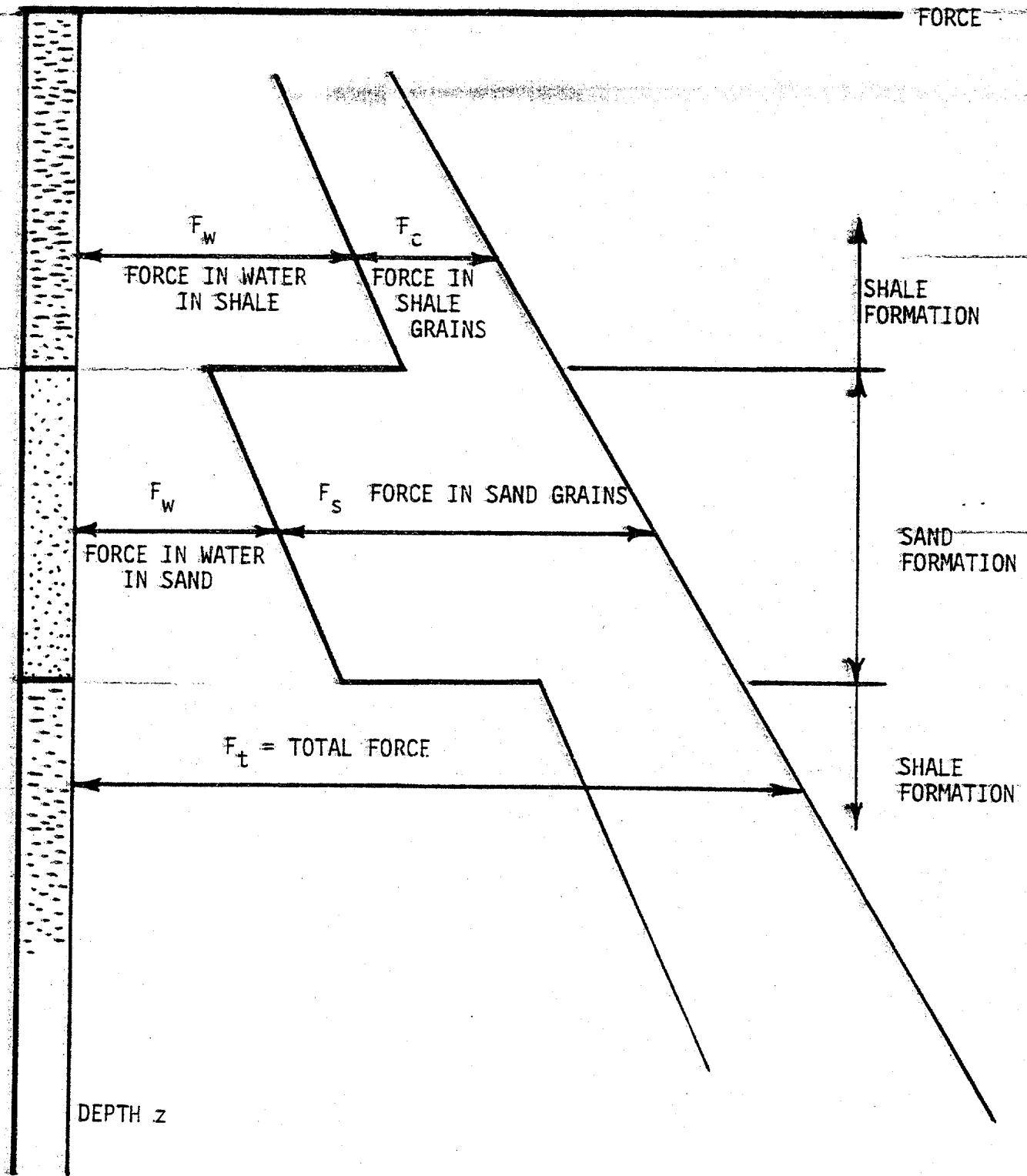
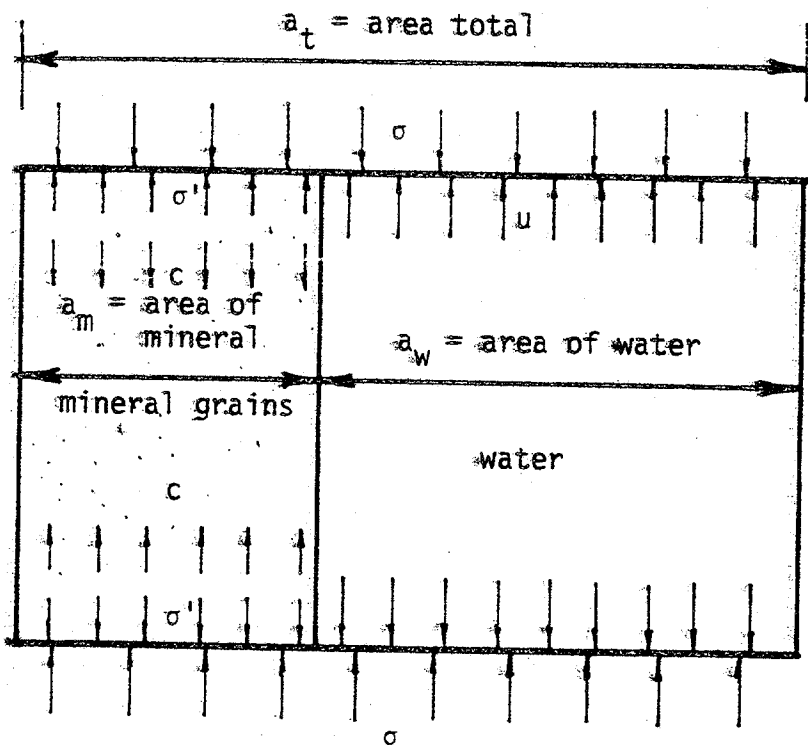


FIG. 2

SHALE, SAND AND WATER FORCES AS A FUNCTION OF DEPTH



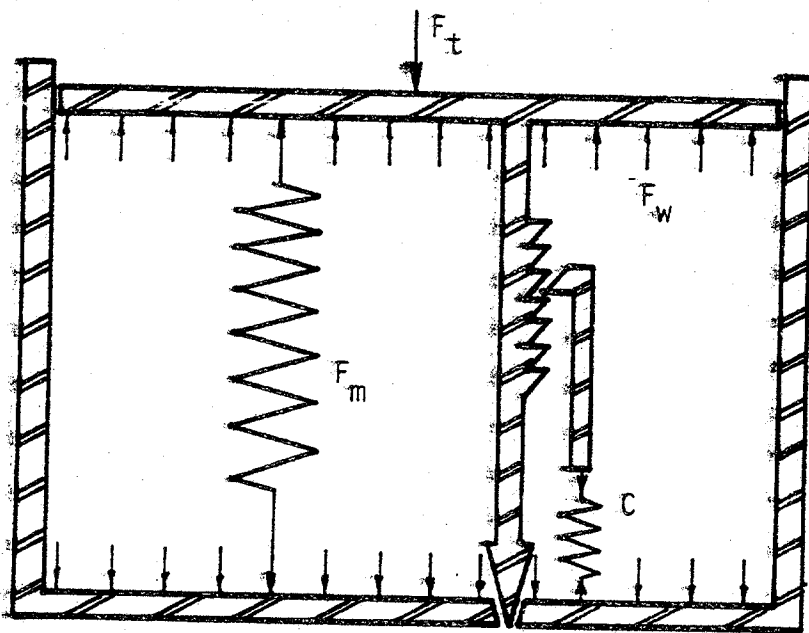
$$a_m + a_w = a_t$$

$$\frac{a_m}{a_t} + \frac{a_w}{a_t} = 1$$

$$A_m = \frac{a_m}{a_t} = 1 - n^E$$

$$A_w = \frac{a_w}{a_t} = n^E$$

} area ratios



$$F_t = \sigma a_t$$

$$F_m = \sigma' a_m$$

$$C = c a_m$$

$$F_w = u a_w$$

$$F_t + C = F_m + F_w$$

or

$$\sigma = (\sigma' + c)(1 - n^E) + u n^E$$

FIG. 3

MECHANISTIC ANALOGY FOR FORCES IN SEDIMENT AND WATER

the area of contact between the mineral grains. The cohesion (plus the attraction) is represented by c acting over the same area of contact between the mineral grains. Cohesion is the internal force that gives soil or rock tensile or shear strength in the absence of any compressive force between mineral grains caused by external forces. The water pressure is represented as u acting over all the area in excess of the contact area between the mineral grains.

Since the sum of the mineral grain contact area a_m and the water area a_w must be equal to the total area a_t , it can be seen that

$$\frac{a_w}{a_t} + \frac{a_m}{a_t} = 1$$

or $A_w + A_m = 1$ Eq. 1

where the A_w and A_m are the area ratios.

The area ratios change as the sediment consolidates into rock. The porosity and the area ratios are not independent for when the porosity is zero, $A_m = 1$ and $A_w = 0$, and when the porosity is one, $A_m = 0$ and $A_w = 1$. Figure 4 shows that the area ratios can be represented as a power law function of the porosity ratio n to give

$$A_w = n^E \text{ and } \dots \dots \dots \text{ Eq. 2}$$

$$A_m = 1 - n^E \dots \dots \dots \text{ Eq. 3}$$

because this function satisfies the required natural boundary conditions. For mathematical reasons porosity ratio n herein is defined as the ratio

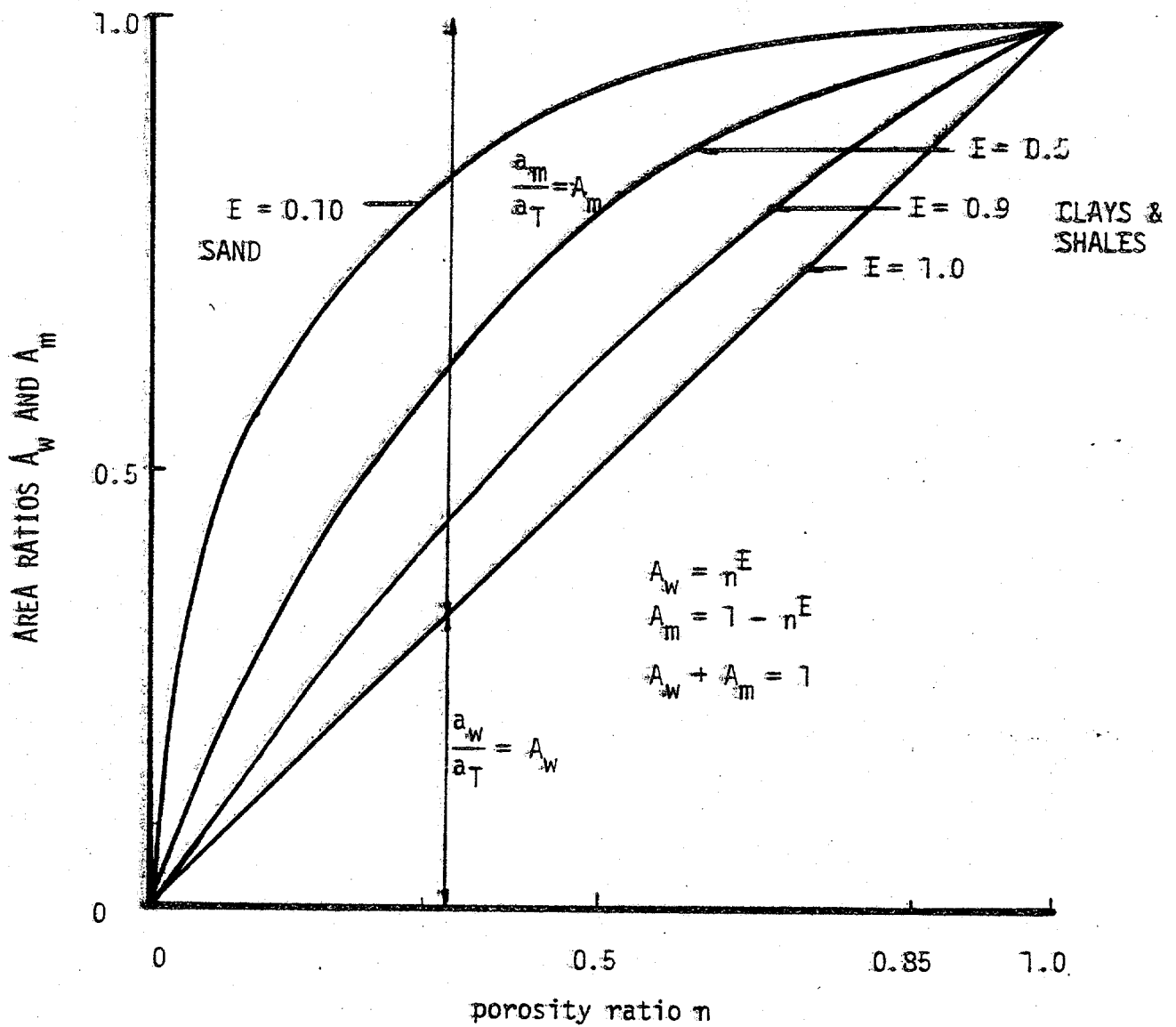


FIG. 4

POWER LAW REPRESENTATION OF THE RATIO OF THE AREA OF THE WATER AND AREA OF THE MINERAL TO THE TOTAL AREA AS A FUNCTION OF POROSITY RATIO

of the volume of the voids divided by the total volume or a number always less than 1 rather than a percentage.

More than likely, for sands E is very small and A_m approaches zero for the high porosity clean sand. For clays and shales E is probably close to one, because as shown by Bennett et al. (7), the cross sectional area ratio of the water in a clay sediment is the same as the porosity determined on a volumetric basis. It is also possible that as the structure of a thixotropic clay suddenly changes the value of E changes.

The bottom diagram of Figure 3 shows how the forces within the sediment might be represented with a typical text book piston-water filled cylinder-compression spring analogy. The second tension spring-ratchet is used to represent the cohesion that develops as the clay mineral is forced into closer contact. The cohesion prevents very much rebound or change in porosity as the sediment is unloaded and gives the soil or rock tensile strength when completely unloaded. The needle valve at the bottom can be used to represent the permeability of the sediment and its changes as the porosity decreases. The porosity is represented by the height of the cylinder.

Since equilibrium requires the total force to be equal to the mineral force plus the water force then

$$\sigma (a_t) = (\sigma' + c)(a_m) + u a_w \dots \dots \dots \text{Eq. 4}$$

by dividing through by the a_t and using the power law representation for the area ratios then

$$\sigma = (\sigma' + c)(1 - n^E) + u n^E \dots \dots \dots \text{Eq. 5}$$

- where σ = total vertical stress
 σ' = contact compression stress transmitted through the mineral
 c = cohesion between the mineral grains

For geostatic conditions, equilibrium also requires that the total vertical stress times the total horizontal area of one unit be equal to the weight of the overburden above the unit area.

Combining the equilibrium condition with Equation 5 it can be seen that

$$(\sigma' + c)(1 - n^E) + un^E = \int_0^Z \gamma_T dz \dots \dots \dots \text{Eq. 6}$$

If for some reason the total force in the soil is small and approaches zero so that the water carries most of the load it can be seen that the pore pressure

$$u = \frac{1}{n^E} \int_0^Z \gamma_T dz \dots \dots \dots \text{Eq. 7}$$

Since both n and E must always be less than one, the term n^{-E} must always be greater than 1. Therefore, the pore pressure can exceed the overburden stress with geostatic conditions and equilibrium still be maintained. However, it should be noted that the pore pressure in sand and sandstone with a porosity ratio of 0.3 and with an E value of 0.3, the maximum pore pressure would be about 1.44 times the overburden stress. For a clay or shale with a porosity ratio of 0.3 and an E value of 1 then

the maximum pore pressure would be about 3.33 times the overburden stress. In each case the Terzaghi effective stress, which is the difference between the total stress and the pore pressure, would be negative, whereas the effective force in the mineral only approaches zero.

In oil field practice, formation pore pressure is determined by measuring the pressure in the drilling fluid. It is assumed that formation pore pressure is the same if there is no flow from the formation to the bore hole or vice versa. It is usually assumed that these pore pressure measurements are only meaningful for the very porous formations such as sand and sandstones where a difference in the pressures will cause a flow large enough for detection. In the almost impermeable formation such as clay and shale the formation pore pressure might be either greater or less than the drilling fluid pressure but the very small flow rates that would develop could not be detected and ages would be required for pore pressure equilibrium. However, there is probably a limit on the pore pressure. As Dave Powley has pointed out it is probably the pressure required to cause a natural hydrofracture.

It is well documented that many deeply buried rock formations in the Gulf Coast region of Texas and Louisiana, 800 miles long, are overpressured. Pore pressures of about 1.4 times the overburden stress have been measured (13). Abnormal pressures have also been measured in Pakistan, Iran, Papua and the U.S.S.R. When blowouts occur no one knows what the original formation pressure was; however, it must have been high enough to accelerate the whole column of drilling fluid. Over 60 mobile offshore drilling rigs have been involved in blowout accidents worldwide and there have been 154 permanent Gulf Coast drilling platforms involved in blowout accidents (33)(25). Overpressures and blowouts are worldwide occurrences.

Many have thought that only the deep rock formations are overpressured but this is debatable since an offshore blowout occurred off the Louisiana coast at a depth of 184 ft below the mudline, as Dave Powley of Amoco Oil Co. has pointed out. In fact, 3 different sets of pore pressure measurements by William Bryant of the Oceanography Department and Wayne Dunlap of the Civil Engineering Department, Texas A&M University, Richard Bennett of the NOAA Marine Geology and Geophysics Lab, Miami, Florida, and by Tom Hamilton of FUGRO Gulf Engineering, Houston, Texas, in the Mississippi delta both on shore and off shore show that at depths of 20 ft and 40 ft below the mudline the pore pressure substantially exceeds the overburden stress (8).

4. EXPERIMENTAL WORK - COMPRESSIBILITY, PERMEABILITY AND HEAT CONDUCTIVITY

A new high pressure stainless steel progressive burial simulator has been designed, constructed and calibrated. Figure 5 through Figure 9 shows the design of the equipment. The ocean bottom sediment is compressed and heated to model the effect of both the overburden pressure and the thermal gradient. The maximum vertical stress is 10,000 psi and the maximum temperature is 200^oF. The diameter of the sample is 2.5 inches. The sediment is loaded or unloaded and heated incrementally and allowed to consolidate and reach equilibrium before testing. The rate of change of porosity is measured by the rate of height change and this is checked against the rate of flow of water from the sample.

Figure 5 shows the consolidometer and Figure 6 shows the lever system loading the consolidometer. Figure 7 shows a schematic of the consolidometer and Figure 8 is a schematic of the measuring system for the consolidometer system.

After reaching equilibrium the permeability and heat conductivity is measured. The coefficient of earth stress at rest is also measured continuously during the consolidation process. The sample is confined by a 0.03 inch thick stainless steel cylinder that is strain gauged in the horizontal direction. The thin stainless steel cylinder is confined by water inside the thick stainless steel outside cylinder. As the strain gauges register, water is forced in to null the strains. The measured water pressure simulates the lateral earth stress.

The permeability is measured directly by forcing sea water through the sample with various hydraulic gradients. The maximum hydraulic gradient

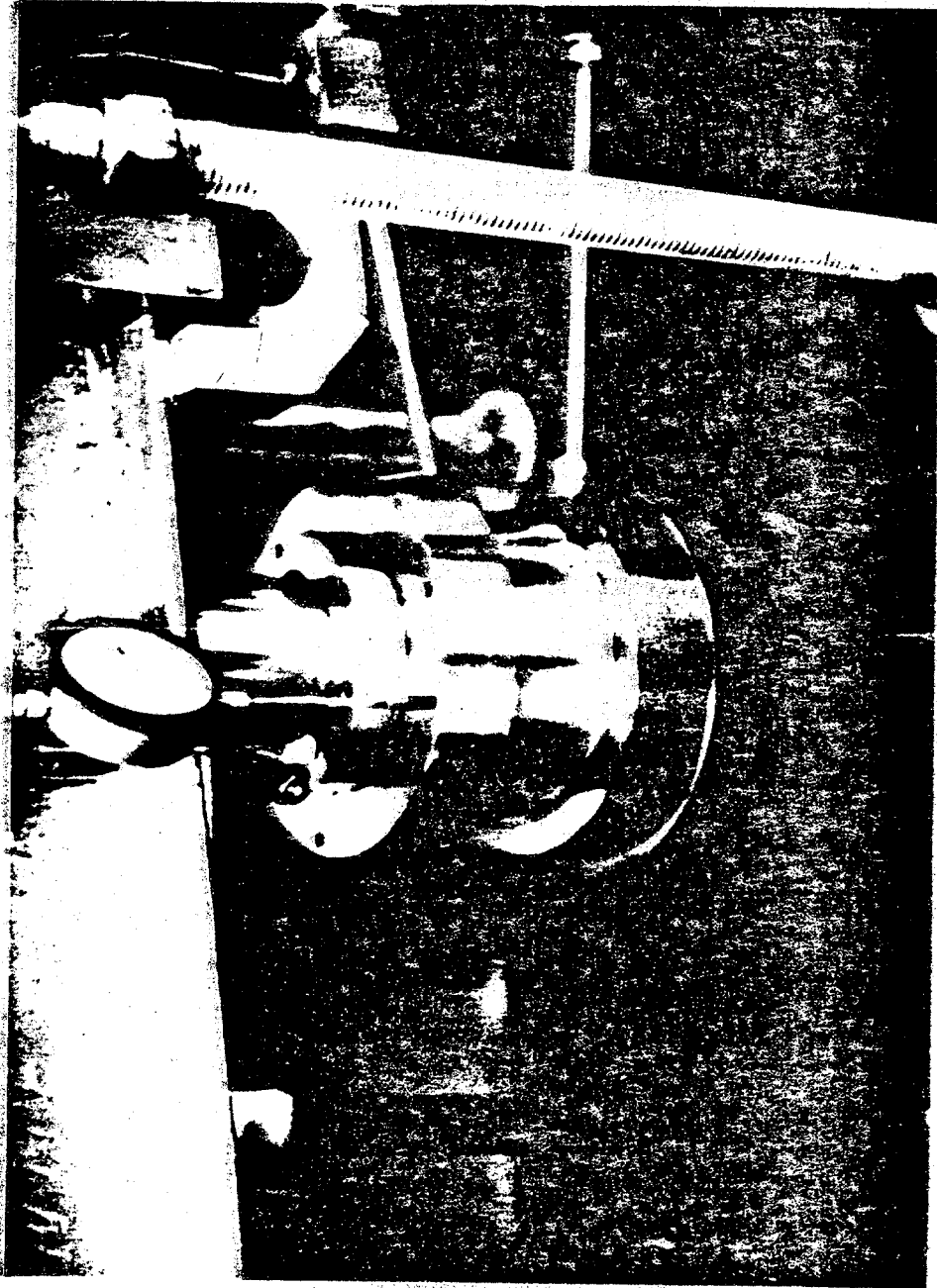


FIG. 5 - High pressure stainless steel consolidation meter

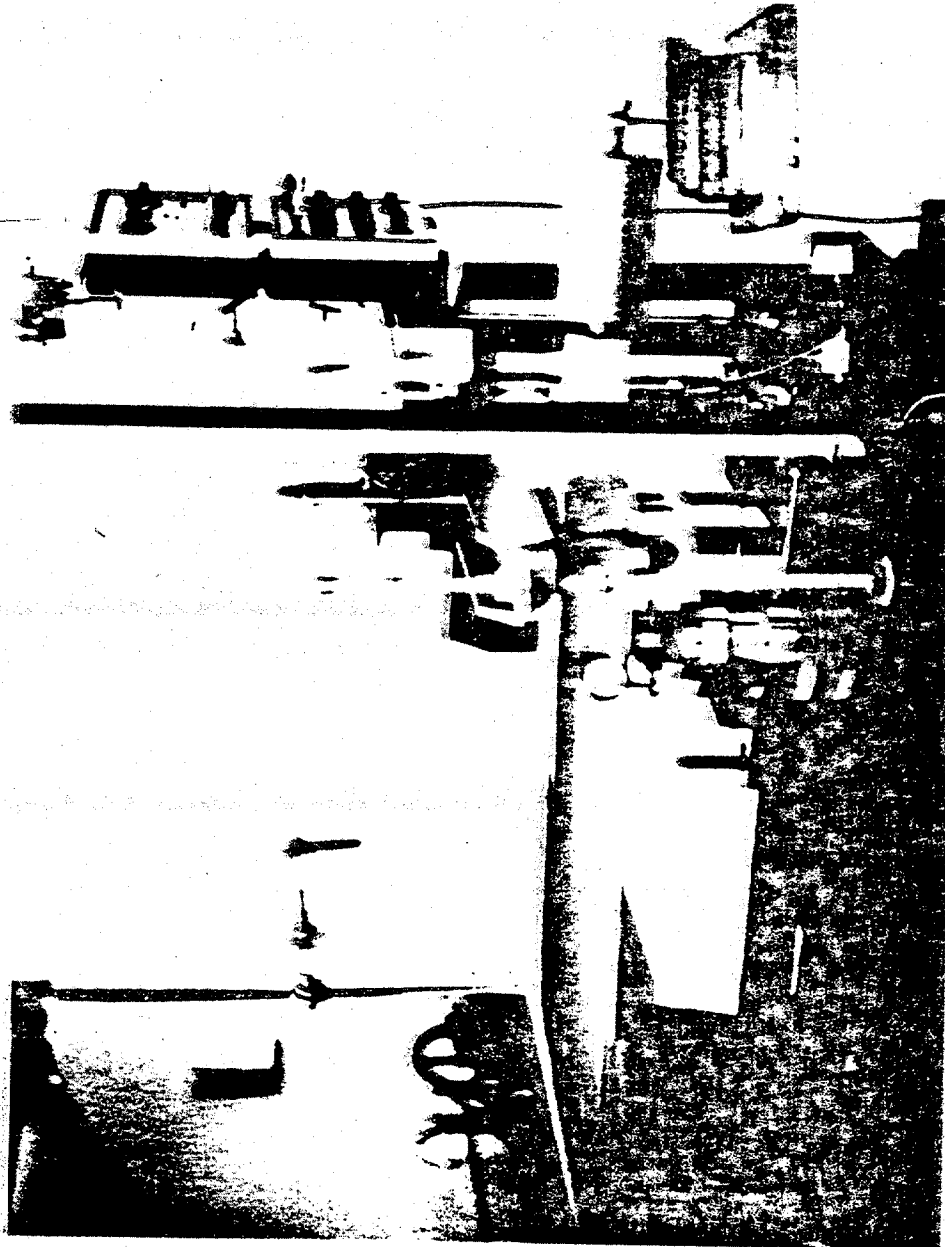


FIG. 6 - Lever loading system and consolidometer

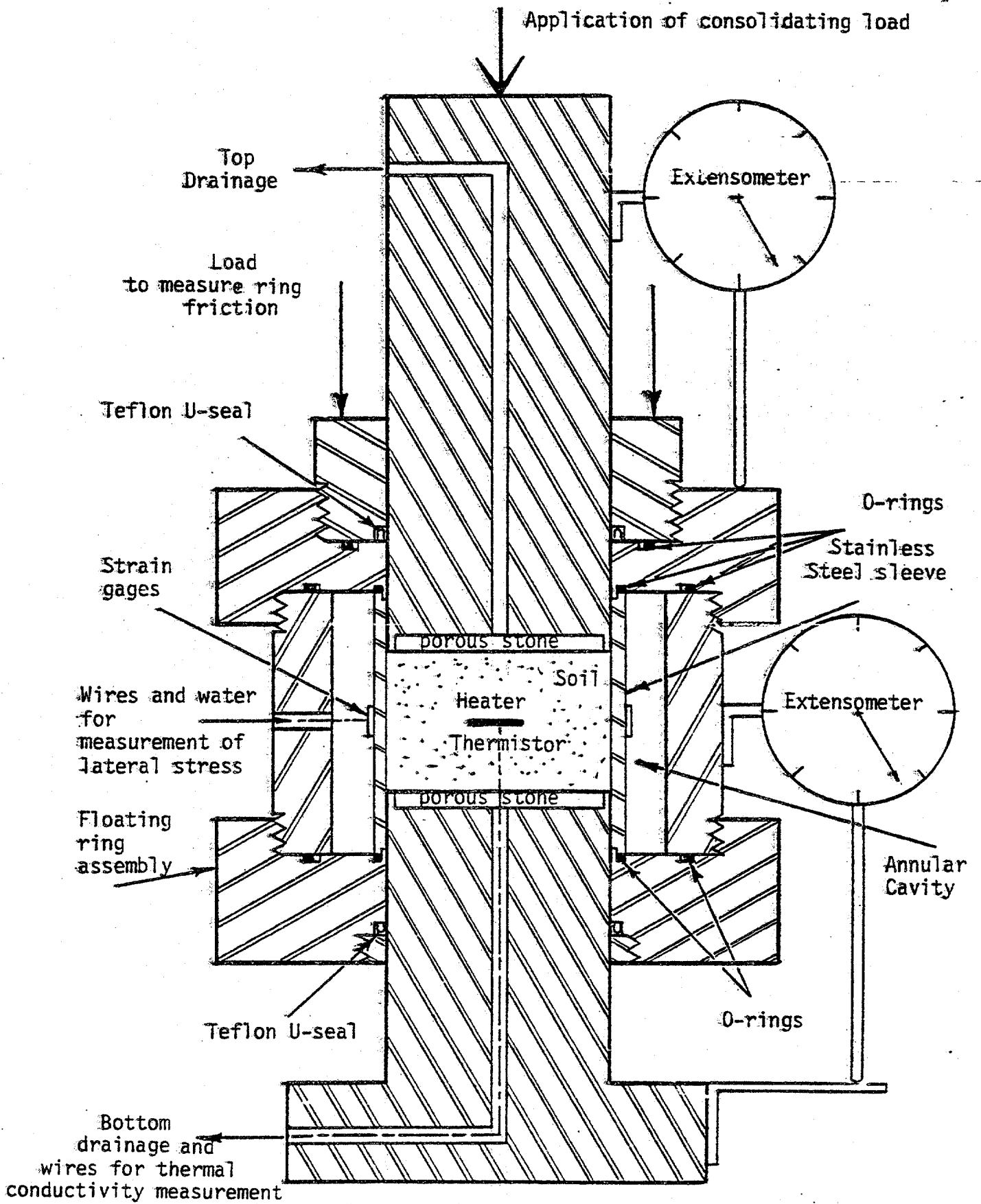


FIG. 7 - Schematic of High Pressure Stainless Steel Consolidometer

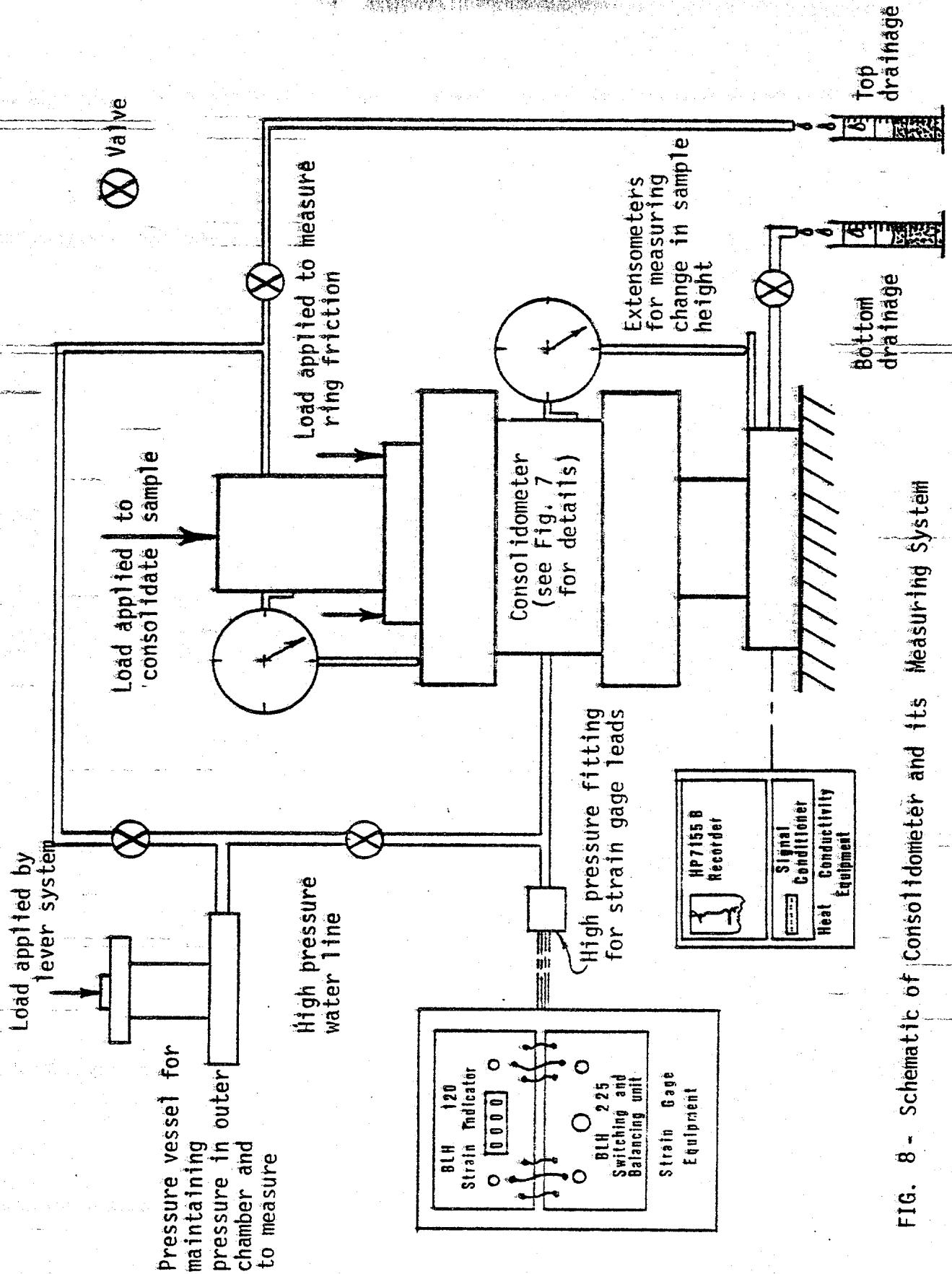


FIG. 8 - Schematic of Consolidometer and its Measuring System

used has been the consolidation stress divided by the length of the sample.

The heat conductivity is measured using the transient method. A tiny heating element and a thermister is embedded in the center of the sample. Figure 9 shows the heat conductivity transducer and the recording equipment. After an increment of consolidation is complete a constant amount of power is supplied to the heating element. The temperature change is recorded as a function of time during the heating phase. The transient solution for the change in temperature $\Delta\theta$ of a spherical heat source of radius r embedded in an infinite media is given in Carslaw and Jaeger (10) as

$$\Delta\theta = \frac{q}{4 \cdot \pi \cdot k_h \cdot r} \left\{ 1 - e^{-\left[\frac{\alpha t}{r^2}\right]} \cdot \text{erfc} \left[\frac{\alpha t}{r^2}\right] \right\} \dots \dots \dots \text{Eq. 8}$$

where q = rate of energy output from the sphere

t = time

k_h = thermal conductivity

$\alpha = \frac{k_h}{\rho C_v}$ = thermal diffusivity of the media

ρ = mass density

and C_v = specific heat of the media.

The term "erfc" is the complimentary error function and is the solution to the integral

$$\text{erfc} \sqrt{\frac{\alpha t}{r^2}} = \frac{1}{2\pi} \int_{\lambda}^{\infty} e^{-\beta^2} d\beta \dots \dots \dots \text{Eq. 9}$$

$$\lambda = \sqrt{\frac{\alpha t}{r^2}}$$

where $\beta = \frac{r}{2} \sqrt{\alpha t}$. The solution to this integral can be found in various

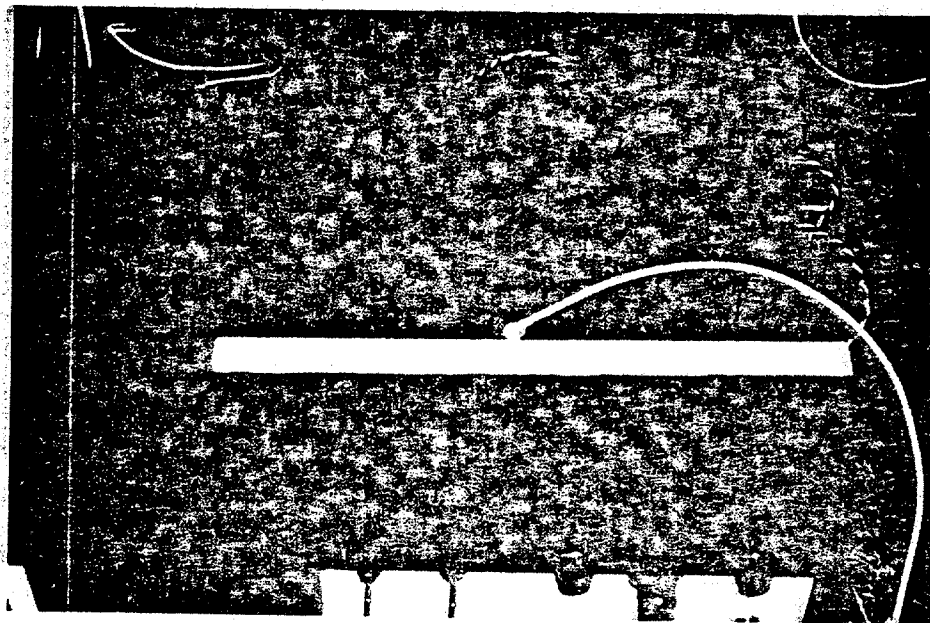
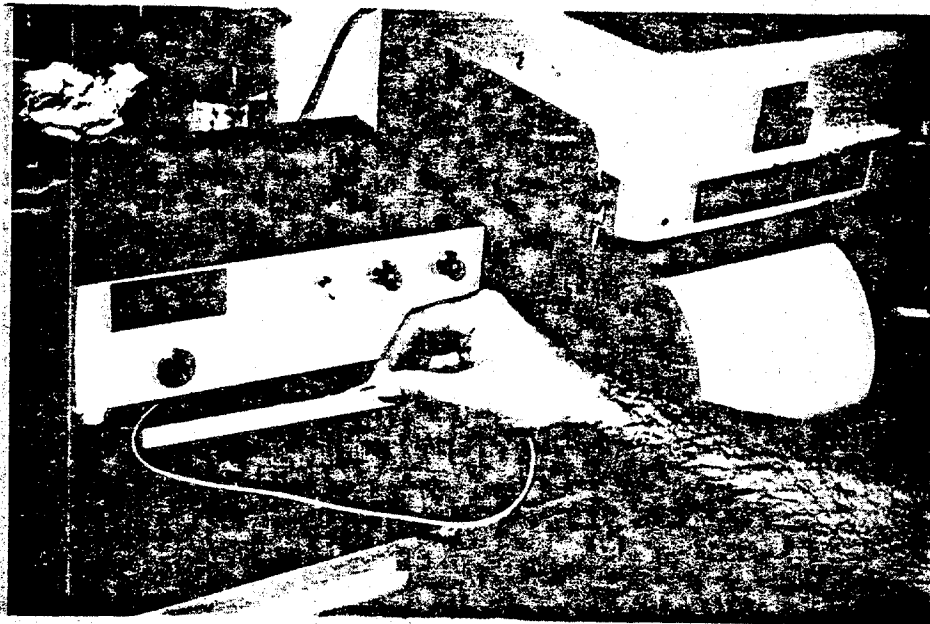


FIG. 9 - Heat Conductivity Transducer and Recording Equipment

math and statistics books.

The recorded temperature vs time test results and Equation 8 make it possible to calculate the thermal conductivity k_h when the specific heat C_v , the radius of the spherical heater r and the mass density ρ is known. A computer program has been written to calculate the conductivity by iteration methods because of the difficulty in inverting the solution to the transient heat equation for spherical dissipation.

The samples were reconstituted by mixing them with sea water to get the maximum porosity to model the physical state at the ocean bottom. The mineralogy and the Atterberg limits were determined for type of sediment before and after each set of loading and unloading tests.

5. EXPERIMENTAL RESULTS

Compressibility

The materials originally tested are described in Table I. It gives the Atterberg limits and the mineralogy of the sediments. The temperature was 22°C. By plotting the force in the mineral against the porosity ratio on a log-log plot, as shown in Fig. 10, it has been found that a power law fits the data very well giving

$$\sigma - un^E = An^B \dots \dots \dots \text{Eq. 10}$$

where σ = total vertical stress acting over a unit area,

u = pore pressure,

n = porosity ratio,

E = area constant,

A = intercept of function when $n = 1.0$,

and B = slope of function.

The expression on either side of the equality in Equation 10 is the force in the mineral which has an area of $1-n^E$ when the total area is unity.

The compressibility coefficients A and B are given in Table 2 for the different sediments tested. The power law can be seen to be a good representation of the compressibility because in fitting the data the coefficient of determination is always equal to or greater than 0.92.

Sand was found not to be very compressible, although the very high stresses did cause some grain breakage, degradation and comminution. All of the data presented are for samples that have been ground up and mixed

TABLE 1 - Atterberg Limits and Mineral Analysis of Sediment

	Sample		Virginia	Mississippi Delta	Campeche	Hawaii	South China Sea
	Test						
Atterberg Limits	Liquid limit	before	59.3	113.2	61.4	92.5	69
		after			67.5	96.7	68
	Plastic limit	before	39.3	32.8	26.3	35.2	37
		after			23.4	34.5	30
Mineral Constituents by X-ray diffraction	Smectite	before		61.0	52.0	54.0	9.0
		after			52.0	57.0	10.0
	Illite	before	52.0	17.0	48.0	22.0	43.0
		after			42.0	21.0	42.0
	Kaolinite	before	36.0	17.0		24.0	27.0
		after				22.0	31.0
	Chlorite	before		5.0			21.0
		after				6.0	17.0
	Vermiculite	before	7.0				
		after					
	Quartz	before	5.0				
		after					

NOTE: The liquid limit and plastic limit are Atterberg limits. These are moisture contents defined as the weight of water divided by the weight of the mineral. These tests are described in ASTM D423-61T and D424-59 (2).

The six minerals listed are the percent of the total sediment measured by X-ray diffraction. See Gibbs, R. J., 1970

before - denotes test results before consolidation.

after - denotes test results after consolidation to 10,000 psi at room temperature

CONSOLIDATION STRESS, $\sigma - un^E$ (psi)

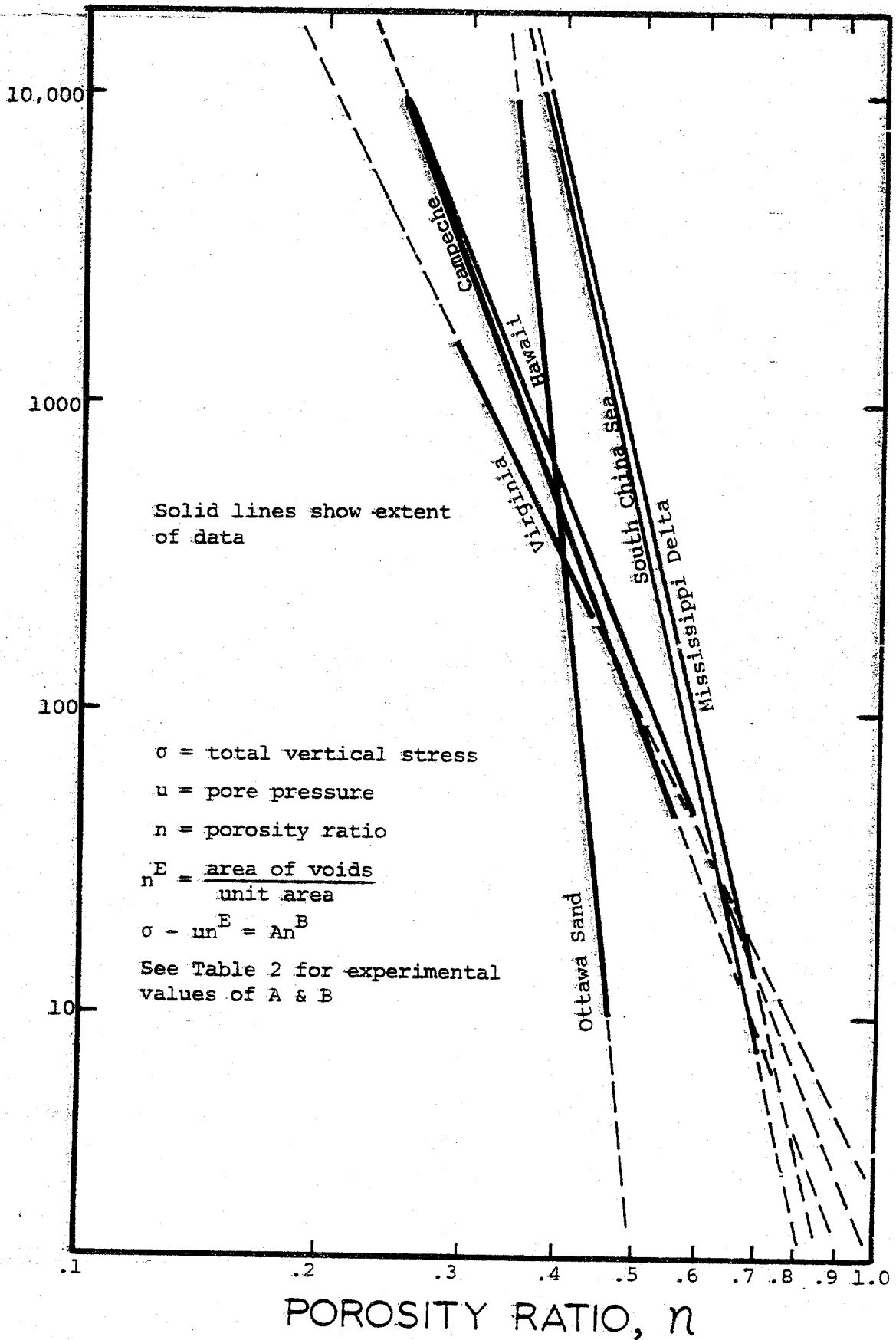


Fig. 10 - Plot of consolidation stress as a function of porosity ratio.
(Laboratory test results)

TABLE 2 - Constants for Consolidation and Permeability "Power Law" Equations

ORIGIN OF SEDIMENT	CONSOLIDATION			PERMEABILITY		
	Constants			Constants		
	A (psi)	B	r ²	C (cm/sec)	D	r ²
Virginia	1.799 x 10 ⁰	- 5.50	1.00	1.768 x 10 ⁻²	18.41	0.99
Mississippi Delta	3.484 x 10 ⁻¹	-11.21	0.97	2.4984 x 10 ⁻⁵	18.17	0.98
Campeche	2.728 x 10 ⁰	- 6.73	0.92	7.2275 x 10 ⁻⁷	6.610	0.95
Hawaii	3.592 x 10 ⁰	- 5.71	0.96	8.2356 x 10 ⁻⁸	6.525	0.94
South China	3.721 x 10 ⁻¹	-10.10	0.98	4.6436 x 10 ⁻⁶	10.18	0.98
Ottawa Sand	7.376 x 10 ⁻⁸	-23.55	0.94	2.0053 x 10 ⁻⁴	.630	1.00

Consolidation: $\sigma - un^E = An^B$ (psi) = 144 An^B (lbs/sq ft) = $6.894 \times 10^3 An^B$ pascals

Permeability: $k = Cn^D$ (cm/sec) = $10^6 Cn^D$ (ft/year) = $3.048 \times 10^5 Cn^D$ m/year

$0 < n < 1$ where $n = \text{porosity ratio} = \frac{\text{volume of voids}}{\text{total volume}}$

r^2 = coefficient of determination to measure goodness of fit of data by assumed "power law." Note that $0 \leq r^2 \leq 1$, and if $r^2 = 1$, there is a perfect fit. See Draper and Smith, (11).

with sea water so as to start at the highest porosity possible. Some of the samples were from the ocean bottom; others were taken by the Glomar Challenger deep ocean drillship.

Further testing has also shown that the compressibility coefficients A, B, and B_u are very sensitive to temperature. Results of new tests on kaolinite show that at a temperature of 22°C

$$A = 2.313 \times 10^{-3} \text{ psi}$$

$$B = - 16.112$$

and for a temperature of 90°C

$$A = 6.903 \times 10^{-1} \text{ psi}$$

$$B = - 6.4744$$

Unloading

Further experimentation has shown that the sediment does not recover its original height or porosity ratio when unloaded. As shown in Fig. 11, for kaolinite clay, the sediment unloads and reloads along a steeper function than the original loading. The slope of the unloading function seems to be a constant and independent of the minimum porosity ratio (n_0) developed during its history. The material also seems to reload along nearly the same path until the minimum porosity ratio n_0 is reached. Then the material follows the original loading function. During unloading and reloading, the total force in the mineral can be described by another power law like Equation 10, where

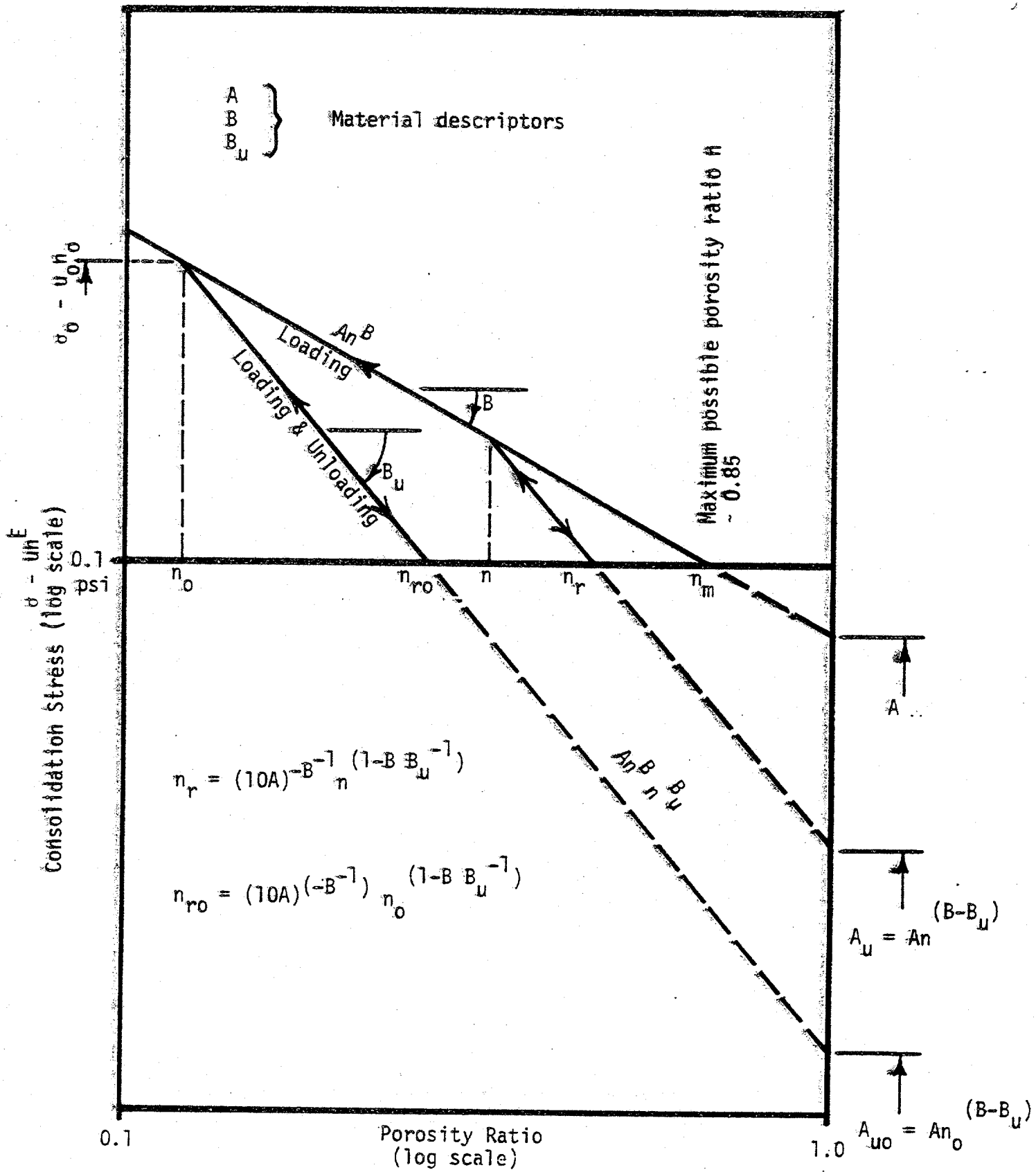


FIG. 11 - Typical Loading and Unloading Function for Marine Sediment in Uniaxial Compression

$$(\sigma - un^E)_u = A_u n^{B_u} \dots \dots \dots \text{Eq. 11}$$

$$n \geq n_0$$

Again each side of the equality is the total force in the mineral. The unloading compressibility coefficients apply for both unloading and reloading as long as $n \geq n_0$. At the minimum porosity n_0 both loading and unloading functions must describe the material therefore

$$A n_0^B = A_u n_0^{B_u}$$

Solving for A_u yields

$$A_u = A n_0^{(B-B_u)} \dots \dots \dots \text{Eq. 12}$$

now the unloading function becomes

$$(\sigma - un^E)_u = A n_0^{(B-B_u)} n^{B_u} \dots \dots \dots \text{Eq. 13}$$

The material can never be completely unloaded because of gravity. Therefore, the porosity ratio that can be recovered n_r can be computed for a very small total force in the mineral of say, 0.1 pounds when the cross sectional area of the water and the mineral is one sq. in. Therefore, Equation 13 becomes

$$0.1 = A n_0^{(B-B_u)} n_r^{B_u} \dots \dots \dots \text{Eq. 14}$$

Solving for the porosity ratio that can be recovered n_r produces

$$n_r = \left[\frac{0.7}{A} n_0 B_u^{-B} \right]^{(B_u^{-1})}$$

or
$$n_r = (10A)^{(-B_u^{-1})} n_0^{(1-B B_u^{-1})} \dots \dots \dots \text{Eq. 15}$$

If the material has never been unloaded then $n_0 = n$ and the recoverable porosity ratio becomes

$$n_r = (10A)^{(-B_u^{-1})} n^{(1-B B_u^{-1})} \dots \dots \dots \text{Eq. 16}$$

Since the porosity ratio is a direct measure of the vertical strain since deposition the rate of recoverable strain becomes

$$\frac{\partial n_r}{\partial t} = (10A)^{(-B_u^{-1})} n^{(1-B B_u^{-1})} \frac{\partial n}{\partial t} \dots \dots \dots \text{Eq. 17}$$

Rate of Change of Strain Energy

The input rate of change of strain energy can be written as

$$\sigma' \dot{\epsilon} = \frac{An^B}{1-n} \frac{\partial n}{\partial t} \dots \dots \dots \text{Eq. 18}$$

and the recoverable rate of change of strain energy can be written as

$$\sigma' \dot{\epsilon}_r = \frac{An^B}{1-n} \left[(10A)^{(-B_u^{-1})} n^{(1-B B_u^{-1})} \right] \frac{\partial n}{\partial t} \dots \dots \dots \text{Eq. 19}$$

The difference in these two terms is the dissipation or the stress power

that produces heat. It is

$$\sigma' \dot{\epsilon} = \sigma' \dot{\epsilon}_r = \frac{An^B}{1-n^E} \left[1 - (10A)^{-B-1} (1-B B_u^{-1}) n^{(-B B_u^{-1})} \right] \frac{\partial n}{\partial t} \quad \text{Eq. 20}$$

The second law of thermodynamics requires that the dissipation always be greater than or equal to zero. This requirement is equivalent to a statement of the entropy principle, and it is sometimes called the Clausius-Planck principle. It should be noted that Eq. 20 is always positive.

Cohesion

In well drilling it is the cohesion that keeps the clay or shale cuttings intact as they are pumped to the surface. The unloading function can be used to study the development of this cohesion that holds the material together after it is unloaded as shown in Fig. 11. From Eq. 5 the force in the mineral can be written as

$$(\sigma - un^E)_u = A_u n_u^B = (\sigma' + c)(1 - n^E) \quad \text{Eq. 21}$$

where

$$(\sigma - un^E)_u < (\sigma - un^E)_o$$

n_o = mineral porosity ratio developed during the history of the material,

c = cohesive stress in the mineral acting on the area $1-n^E$.

The porosity ratio is determined by the mineral stress σ' for both loading and unloading, therefore

$$(\sigma')(1-n^E) = An^B$$

$$\sigma' = \frac{An^B}{1-n^E} \dots \dots \dots \text{Eq. 22}$$

Substituting Equation 22 and Equation 12 into Equation 21 produces

$$An_o^{(B-B_u)} = \left(\frac{An^B}{1-n^E} + c \right) (1 - n^E)$$

or

$$c = \frac{An_o^{(B-B_u)} - An^B}{1-n^E} = \frac{A(n_o^{B-B_u} - n^B)}{1-n^E} \dots \dots \dots \text{Eq. 23}$$

The cohesive stress, c, is assumed to act on a horizontal plane in a vertical direction. The cohesive stress in other directions is probably different because of the anisotropy of the particle orientation. It should be noted that the calculated value of the cohesion is always negative or tensile.

The maximum cohesion would develop if the total stress could somehow be made tensile to the point that σ' approaches zero, say 0.1 psi, then just before tensile failure Equation 23 would require that

$$An_o^{(B-B_u)} n^B = 0.1 + c (1-n^E)$$

and

$$c_{\text{max}} = \frac{An_o^{(B-B_u)} n^B - 0.1}{1-n^E} \dots \dots \dots \text{Eq. 24}$$

Pore Pressures

The unloading function can also be used to compute the minimum possible pore pressure to be expected while drilling. By measuring the porosity ratio of the intact cuttings n_{ro} collected from the circulated drilling

fluid, the minimum value of n_0 can be estimated as shown in Fig. 11.

Solving for n_0 in Equation 14 gives

$$n_0 = (10A)^{\frac{(B-B_u)}{n_{ro}}} (B B_u - B_u^2) \quad \text{Eq. 25}$$

where n_0 is the minimum possible porosity ratio for the mineral in situ.

Therefore, by Equation 10

$$\sigma - un^E \leq An_0^B \quad \text{Eq. 26}$$

or by solving for the pore pressure u then

$$u \geq \frac{\sigma - An_0^B}{n^E} \quad \text{Eq. 27}$$

Substitution of Equation 25 into Equation 27, assuming $E=1$ and taking the minimum possible value of n as n_0 it can be seen that

$$u_{\min} = \sigma(10A)^{\frac{(B_u-B)}{n_{ro}}} (B_u^2 - B B_u) - A(10A)^{\frac{(B-B_u)(B-1)}{n_{ro}}} (B B_u - B_u^2)(B-1) \quad \text{Eq. 28}$$

In order for the pore pressure to exceed this minimum value there must have been unloading. This might occur through hydrofracture or erosional removal of overburden.

As Dave Powley of Amoco Oil Co. has suggested the maximum pore water pressure to be expected is the natural hydrofracture pressure. Since hydrofracture can occur by several mechanisms, there is need to study these mechanisms in order to determine the maximum possible pore pressure.

Permeability

Direct measurements of permeability show that Darcy's law describes the steady state flow in clays. The permeability data can also be described by a power law function of porosity. This function shows that the permeability decreases many orders of magnitude faster than the porosity decreases. The permeability, k , may be described as

$$k = Cn^D \dots \dots \dots \text{Eq. 29}$$

where C and D are constants for each different type of sediment. Typical test results are given in Fig. 12 and the permeability factors are also given in Table 2.

Further testing on kaolinite has shown the permeability coefficients are influenced by temperature. This was expected because sea water becomes less viscous as it is heated. For kaolinite, at 20°C , the power law permeability coefficient, C , was 7.734×10^{-7} cm/sec and the exponential coefficient, D , was 6.40. At 90°C C was 2.012×10^{-6} and D was 5.4188.

Thermal Conductivity and Specific Heat of Sediment

The thermal conductivity for various sediments as determined from a literature survey is shown in Fig. 13. Tests on kaolinite are shown in Fig. 14. The kaolinite test results are much lower than the values published in the literature by a factor of about 2. Most of the published values were determined by a needle probe that measured the horizontal conductivity by inserting it down the axial center of a cylindrical core. Penner has shown that clays have anisotropic thermal conductivities

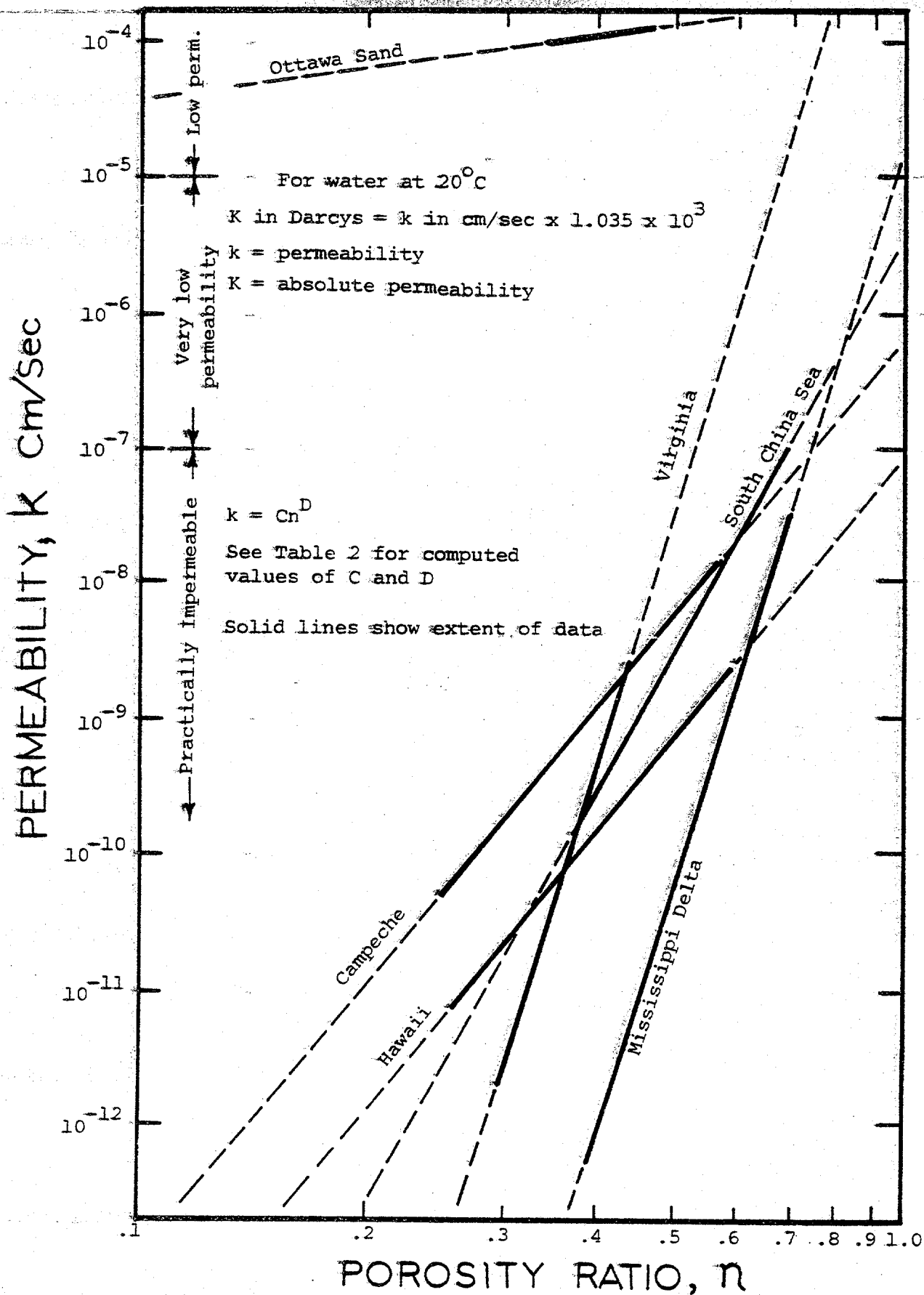


Fig. 12 - Plot of salt water permeability as a function of porosity ratio. (Laboratory test results)

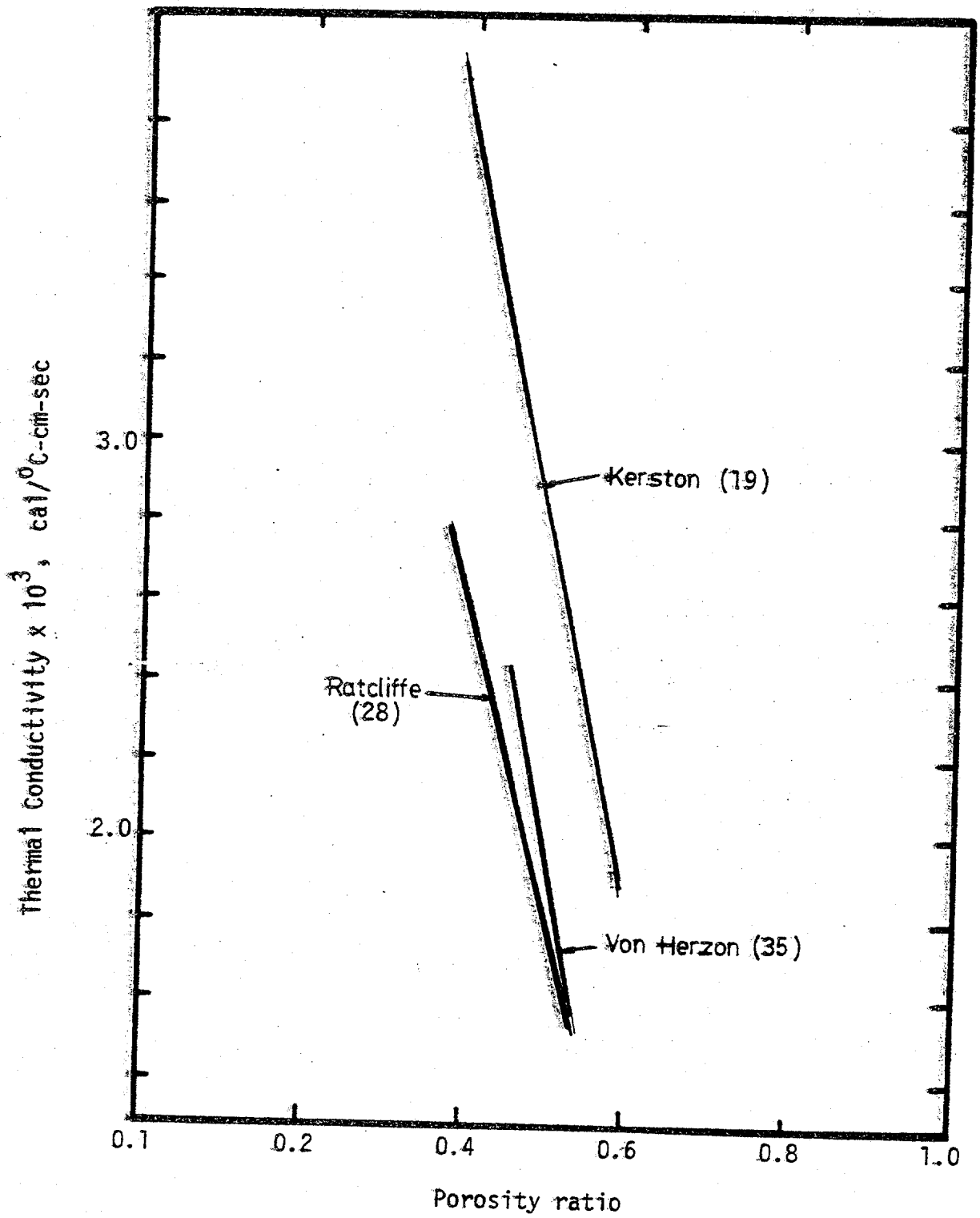


FIG. 13 - Thermal Conductivity of Various Sediments versus Porosity Ratio from the Literature

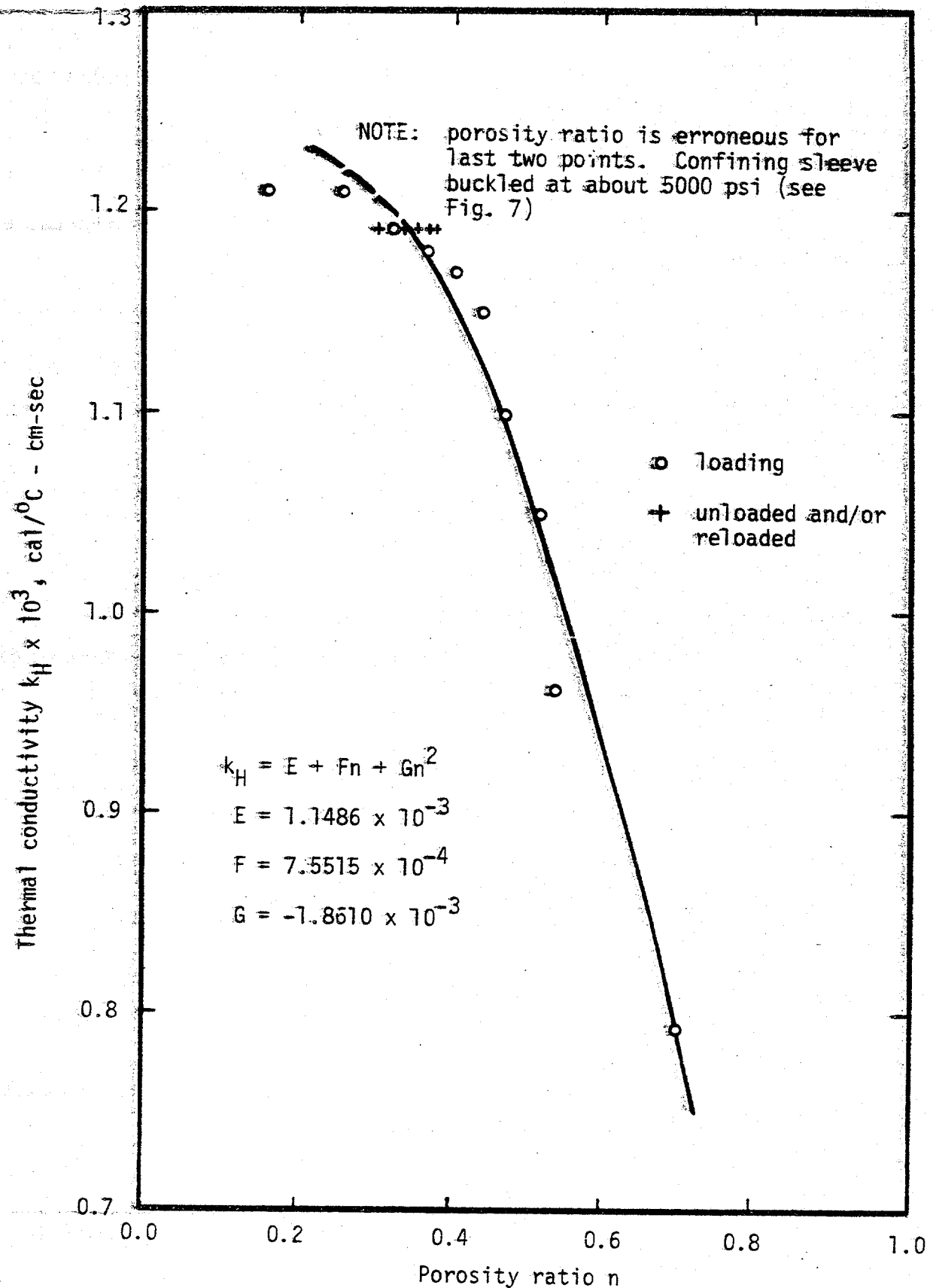


FIG. 14 - Laboratory Thermal Conductivity of Kaolinite measured during Consolidation

because of their anisotropic particle arrangement (26). He found the horizontal conductivity about 1.7 times the vertical conductivity at shallow depth. These kaolinite test results are for the thermal conductivity in the vertical direction in highly compressed sediments with a high degree of horizontal particle arrangement. This may be an explanation for a difference in these test results and in the values that have been found by other investigators using different test equipment, different minerals and different measurement direction.

It should be noted that the last two porosity ratios in Fig. 14 are probably in error. It was found, after the test was over, that the thin sleeve that confined the sample buckled with the high pressure. The porosity ratios were calculated from the height of the sample assuming no lateral deformation. With buckling there was lateral deformation and the last two porosity ratios are wrong. Table 3 shows the load, porosity ratio and thermal conductivity for the kaolinite and Ottawa sand.

The thermal conductivity can be represented as parabolic function of the porosity ratio as

$$k_h = E + Fn + Gn^2 \dots \dots \dots \text{Eq. 30}$$

where k_h = thermal conductivity of the mineral-salt water system in cal/C⁰ cm/sec.,

n = porosity ratio,

and E, F and G are the coefficients to describe the material.

For kaolinite the test results give

$$E = 1.1486 \times 10^{-3}$$

TABLE 3.-Consolidation Load, Porosity and Thermal Conductivity for Kaolinite Clay and Ottawa Sand.

Material	Consolidation Load (psi) ($\sigma - An^E$)	Porosity ratio n	Thermal Conductivity k_H (cal/ $^{\circ}$ C-cm-sec)
Kaolinite Clay	0	0.695	0.79×10^{-3}
	63	0.532	0.96×10^{-3}
	99	0.509	1.05×10^{-3}
	206	0.469	1.10×10^{-3}
	350	0.438	1.15×10^{-3}
	637	0.400	1.17×10^{-3}
	1210	0.360	1.18×10^{-3}
	2357	0.311	1.19×10^{-3}
	350 unload	0.325	1.19×10^{-3}
	63 unload	0.371	1.19×10^{-3}
	206 reload	0.368	1.19×10^{-3}
	637 reload	0.347	1.19×10^{-3}
	2357 reload	0.298	1.19×10^{-3}
	4651	0.251*	1.21×10^{-3}
10386	0.147*	1.21×10^{-3}	
Ottawa Sand	Not Loaded		
	dense	0.390	1.39×10^{-3}
	loose	0.360	1.49×10^{-3}

* Porosity ratio based on sample height not correct because sleeve buckled

$$F = 7.5515 \times 10^{-4}$$

and $G = 1.8610 \times 10^{-3}$

The specific heat times the mass density for a unit volume of the sediment can be calculated if the specific heat of both the mineral and the water is known as

$$\rho_T C_{V_T} = n \gamma_0 G_{SW} C_{SW} + (1-n) G_S \gamma_0 C_S \dots \dots \dots \text{Eq. 31}$$

where

ρ_T = total density of the sediment in gm/cc,

C_{V_T} = total specific heat of the sediment in cal/C⁰ gm,

n = porosity ratio,

G_{SW} = specific gravity of the sea water ~ 1.03,

G_S = specific gravity of the mineral ~ 2.65 to 2.74,

C_{SW} = specific heat of the salt water ~ 0.94 cal/C⁰ gm,

and

C_S = specific heat of the mineral ~ 0.18 cal/C⁰ gm.

Equation 31 is a linear function of the porosity ratio n . When $n=1$ it has a value of 0.94 cal/C⁰-gm. When $n=0$ it has a value of 0.18 cal/C⁰-gm.

6. CONSERVATION OF MASS AND DARCY'S LAW -

DERIVATION OF THE PROGRESSIVE BURIAL CONSOLIDATION EQUATION

As the sediment is compressed water must be expelled if mass is conserved and if the mineral particles and the water are incompressible. This requires that the rate at which the mineral is compressed must be equal to the change in the average flow rate of the water through the mineral. The rate at which the sediment is compressed is the change in the porosity ratio with respect to time. If Darcy's law is true for the sediment then the velocity of the water is given by the product of the hydraulic gradient and the coefficient of permeability. Therefore

$$\frac{\partial ki}{\partial z} = \frac{\partial n}{\partial t} \dots \dots \dots \text{Eq. 32}$$

or

$$i \frac{\partial k}{\partial z} + k \frac{\partial i}{\partial z} = \frac{\partial n}{\partial t} \dots \dots \dots \text{Eq. 33}$$

where

k = coefficient of permeability based on the total area,

n = porosity ratio,

t = time,

z = depth,

and i = hydraulic gradient.

The hydraulic gradient is defined as the change in the total head with respect to the direction of flow. Considering flow upward only and taking the total head to be the sum of the pressure head plus the elevation head then,

$$i = \frac{\partial h_t}{\partial z} = \frac{\partial h_p}{\partial z} + \frac{\partial h_e}{\partial z} \dots \dots \dots \text{Eq. 34}$$

h_t = total head

h_p = pressure head

h_e = elevation head

Taking z as increasing downward the elevation head will decrease with depth and the pressure head will increase with depth. Therefore

$$\frac{\partial h_e}{\partial z} = -1 \dots \dots \dots \text{Eq. 35}$$

The pressure head is defined as follows:

$$\gamma_w h_p = u \dots \dots \dots \text{Eq. 36}$$

where γ_w = unit weight of the water

u = pore pressure

Differentiating Equation 36 with respect to z and substituting it and Equation 35 into Equation 34 produces:

$$i = \frac{1}{\gamma_w} \frac{\partial u}{\partial z} - 1 \dots \dots \dots \text{Eq. 37}$$

or $(i+1) \gamma_w = \frac{\partial u}{\partial z}$

Since the hydrostatic pore pressure produces no flow it is the pore pressure in excess of hydrostatic pressure that is of interest. Defining

$$u = U_{ex} + U_H \dots \dots \dots \text{Eq. 38}$$

where u = total pore pressure

U_{ex} = excess pore pressure

$U_H =$ hydrostatic pore pressure

therefore

$$\frac{\partial u}{\partial z} = \frac{\partial U_{ex}}{\partial z} + \frac{\partial U_H}{\partial z} = \frac{\partial U_{ex}}{\partial z} + \gamma_w \quad \text{Eq. 39}$$

Combining Equation 37 with Equation 39 produces

$$\frac{\partial U_{ex}}{\partial z} = i \gamma_w \quad \text{Eq. 40}$$

or

$$i = \frac{1}{\gamma_w} \frac{\partial U_{ex}}{\partial z} \quad \text{Eq. 41}$$

Differentiating Equation 41 with respect to z and substituting it and Equation 41 into Equation 33 produces

$$\frac{k}{\gamma_w} \frac{\partial^2 U_{ex}}{\partial z^2} + \frac{1}{\gamma_w} \frac{\partial U_{ex}}{\partial z} \frac{\partial k}{\partial z} = \frac{\partial n}{\partial t} \quad \text{Eq. 42}$$

if it is assumed that the unit weight of the water γ_w is a constant,

Equation 41 shows that there must be an excess pore pressure gradient for steady state flow and Equation 42 shows that for consolidation and settlement a gradient of the hydraulic gradient is required. When the pore water is hydrostatic there is no excess pore pressure; any change in pressure head is exactly compensated by the elevation head, and therefore there is no flow.

Equation 29 allows the permeability in Equation 42 to be replaced with a function of the porosity ratio n . Differentiating Equation 29 with respect to z and substituting it and Equation 29 into Equation 42 produces

$$\frac{Cn^D \partial^2 U_{ex}}{\gamma_w \partial z^2} + \frac{CDn^{D-1}}{\gamma_w} \frac{\partial n}{\partial z} \frac{\partial U_{ex}}{\partial z} = \frac{\partial n}{\partial t} \quad \text{Eq. 43}$$

When the experimental compressibility relationship, Equation 10, is combined with the equilibrium condition, Equation 6, it is seen that

$$\sigma = An^B + un^E = \int_0^z \{(1-n)(G_s)(\gamma_0) + nG_w\gamma_0\} dz \dots \dots \dots \text{Eq. 44}$$

Solving for u produces

$$u = -An^{B-E} + n^{-E} \int_0^z \{(1-n)G_s\gamma_0 + nG_w\gamma_0\} dz \dots \dots \dots \text{Eq. 45}$$

Using Equation 38, the assumption that E = 1 for clay and shale, and assuming that

$$n^{-E} \int_0^z \{(1-n)G_s\gamma_0 + nG_w\gamma_0\} dz = \int_0^z \left\{ \left(\frac{1-n}{n} \right) G_s\gamma_0 + G_w\gamma_0 \right\} dz \dots \dots \dots \text{Eq. 46}$$

then

$$u_H + u_{ex} = -An^{B-1} + \int_0^z \left\{ \left(\frac{1-n}{n} \right) G_s\gamma_0 + G_w\gamma_0 \right\} dz \dots \dots \dots \text{Eq. 47}$$

differentiation with respect to z yields

$$\frac{\partial u_{ex}}{\partial z} = -A(B-1)n^{B-2} \frac{\partial n}{\partial z} + (n^{-1} - 1) G_s\gamma_0 \dots \dots \dots \text{Eq. 48}$$

A second differentiation with respect to z yields

$$\frac{\partial^2 u_{ex}}{\partial z^2} = -A(B-1)n^{B-2} \frac{\partial^2 n}{\partial z^2} - n^{-2} G_s\gamma_0 \frac{\partial n}{\partial z} \dots \dots \dots \text{Eq. 49}$$

if it is assumed that the product of differentials are small and can be

ignored.

When Equation 48 is combined with Equation 49 and Equation 43 then

$$\frac{A(B-1)C}{G_w \gamma_o} n^{B+D-2} \frac{\partial^2 n}{\partial z^2} + CD \frac{G_s}{G_w} n^{D-2} (1-n-D^{-1}) \frac{\partial n}{\partial z} = \frac{\partial n}{\partial t} \quad \text{Eq. 50}$$

As mentioned before all the coefficients A, B, C and D and even G_w and G_s are all influenced by the temperature.

This last equation is a parabolic quasilinear second order non-homogeneous partial differential equation. The independent variable, the porosity ratio n , is a function of both depth z and time t . It is the controlling differential equation for consolidation, subject to the above assumptions. Such an equation is said to have a unique solution (3).

In the second term on the left hand side of Equation 50, the porosity ratio n is raised to the power of $D-2$. Since D is always greater than 6 as shown by tests and since n is always less than one, the second term could be dropped with little loss in accuracy. Hermes proved that such an equation had a unique solution (17).

If the coordinate system is attached to the mudline and the origin moves as the sediment subsides or new sediment is deposited and if the rate of deposition is constant, then the mechanical processes at any given depth below the mudline will be independent of time. Different materials will be involved at different times at the same depth but stresses are the same and the length of the drainage path is the same. For these conditions the right hand term of Equation 50 vanishes and Equation 50 becomes an ordinary differential equation giving the porosity ratio n as a function of depth z only. The porosity ratio n will be a constant at the mudline.

7. HYDROSTATIC PRESSURE - DEPTH RELATIONSHIPS FOR INTERSTITIAL SALT WATER

As shown by Equation 50 it is the pore pressure gradient in excess of hydrostatic pressure gradient that produces flow through the sediment, and it is the gradient of the gradient of the excess pore pressure that produces consolidation. To compute the excess pore pressure it is necessary to know the hydrostatic pressure that takes into consideration the effect of the thermal gradient.

Figure 15 shows the bottom hole temperature and Figure 16 shows the bottom hole pressure for a number of wells in Brazoria County, Texas to illustrate how temperature and pressure varies with depth in the Gulf Coast region (6).

Figure 17 shows how the thermal gradient based on bottom hole temperature varies over the Gulf Coast region (23).

To determine pore pressures far below the surface it is necessary to consider the effects of temperature and pressure on the specific gravity of salt water.

Equilibrium requires that the hydrostatic pore pressure be determined using the equation:

$$u_H = \int_0^z \gamma_w dz \dots \dots \dots \text{Eq. 51}$$

or,
$$u_H = \int_0^z \gamma_0 G_w dz$$

which can also be written as: $\frac{du_H}{dz} = \gamma_0 G_w$

where G_w is the specific gravity of the salt water and a function of temperature and pressure and u_H is the hydrostatic pore pressure.

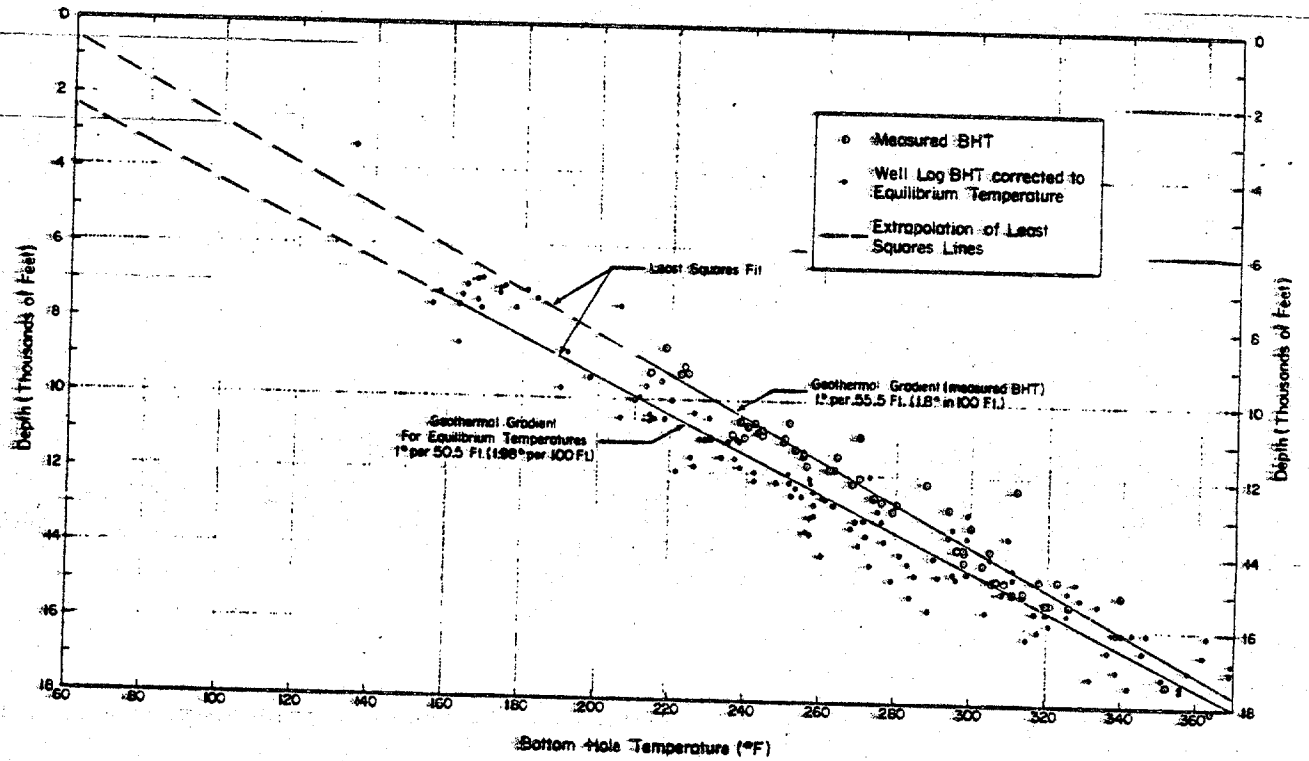


FIG. 15 - Bottom-hole temperature for some wells, Chocolate Bayou Field, Brazoria County, Texas (6).

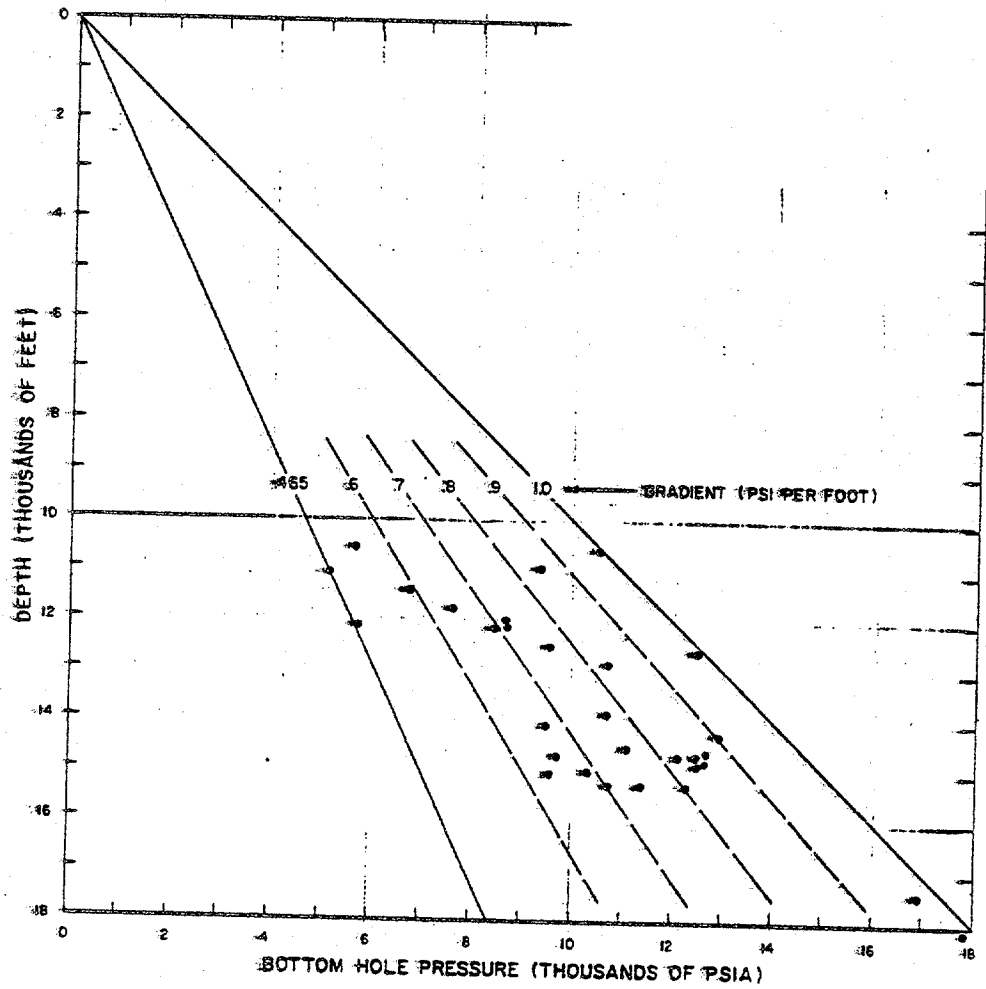


FIG. 16 - Bottom-hole pore pressure for some wells,
Chocolate Bayou Field, Brazoria County, Texas (6).

A non-linear representation of specific gravity of salt water as it relates to temperature and pressure has been developed from data of Fine, Wang and Millero (15), with salinities ranging from 30% to 40%. This representation is as follows:

$$G_w = g(\theta) + f(u) + uh(\theta) \quad \dots \dots \dots \text{Eq. 52}$$

where: $g(\theta) = 1.02651 + 3.91069 \times 10^{-4} \theta - 9.99260 \times 10^{-6} \theta^2 + 1.42754 \times 10^{-8} \theta^3$

$$f(u) = 2.21598 \times 10^{-5} u$$

$$h(\theta) = - 1.76558 \times 10^{-7} \theta + 2.88827 \times 10^{-10} \theta^2$$

u is the pore pressure in psi (0 - 10,000 psi range) and θ is the temperature in degrees centigrade (0 - 200°C range).

A typical linear subsurface temperature profile can be written as:

$$\theta = G + Jz \quad \dots \dots \dots \text{Eq. 53}$$

where G is the surface temperature and J is the thermal gradient.

When this is combined with the above specific gravity equation, the following equation results, which is a function only of pressure and depth:

$$G_w = g_1(z) + f(u) + uh_1(z) \quad \dots \dots \dots \text{Eq. 54}$$

where: $g_1(z) = 1.02651 + 3.91069 \times 10^{-4} (G + Jz) - 9.99260 \times 10^{-6} (G + Jz)^2 + 1.42754 \times 10^{-8} (G + Jz)^3$

$$f(u) = 2.21598 \times 10^{-5} u$$

$$h_1(z) = - 1.76558 \times 10^{-7} (G + Jz) + 2.88827 \times 10^{-10} (G + Jz)^2$$

Performing the necessary algebra and collecting terms yields:

$$G_w = A_0 + A_1 z + A_2 z^2 + A_3 z^3 + (C_0 + C_1 z + C_2 z^2) u \quad \text{Eq. 55}$$

where:

$$A_0 = 1.02651 + 3.91069 \times 10^{-4} G - 9.99260 \times 10^{-6} G^2 + 1.42754 \times 10^{-8} G^3$$

$$A_1 = 3.91069 \times 10^{-4} J - 1.99852 \times 10^{-5} GJ + 4.28262 \times 10^{-8} G^2 J$$

$$A_2 = -9.99260 \times 10^{-6} J^2 + 4.28262 \times 10^{-8} GJ^2$$

$$A_3 = 1.42754 \times 10^{-8} J^3$$

$$C_0 = 2.21598 \times 10^{-5} - 1.76558 \times 10^{-7} G + 2.88827 \times 10^{-10} G^2$$

$$C_1 = -1.76558 \times 10^{-7} J + 5.77654 \times 10^{-10} GJ$$

$$C_2 = 2.88827 \times 10^{-10} J^2$$

Substituting Equation 55 into Equation 51 produces a linear first order differential equation of the form:

$$\frac{\partial u_H}{\partial z} = \{(C_0 + C_1 z + C_2 z^2) u_H + A_0 + A_1 z + A_2 z^2 + A_3 z^3\} \gamma_0 \quad \text{Eq. 56}$$

A fourth order Runge-Kutta finite difference program was written for the AMDAHL 470 V/6 computer to solve this differential equation for different surface temperatures G and different thermal gradients J. The constants used for five different cases were computed and shown in Table 4. Table 5 gives the computed pressures for various depths using the five different cases. The specific gravity of the sea water was then calculated by Equation 55 and is also shown in Table 5.

TABLE 4

Constants in Equation 55 for calculating hydrostatic pressure

CASE	1		2		3		4		5	
	°F	°C	°F	°C	°F	°C	°F	°C	°F	°C
Temp.										
G- Deg.	68	20	68	20	68	20	68	20	68	20
J- Deg./100ft.	0.5	0.28	1.0	0.56	1.5	0.83	2.0	1.11	2.2	1.22
A_0 (No dim.)	1.030		1.030		1.030		1.030		1.030	
A_1 1/ft.	2.379×10^{-8}		4.758×10^{-8}		7.051×10^{-8}		9.430×10^{-8}		1.091×10^{-7}	
A_2 1/ft. ²	-7.163×10^{-11}		-2.865×10^{-10}		-6.294×10^{-10}		-1.126×10^{-9}		-1.316×10^{-9}	
A_3 1/ft. ³	3.134×10^{-16}		2.507×10^{-15}		8.162×10^{-15}		1.952×10^{-14}		2.467×10^{-14}	
C_0 in ² /lb.	1.874×10^{-5}		1.874×10^{-5}		1.874×10^{-5}		1.874×10^{-5}		1.874×10^{-5}	
C_1 in ² /lb. ft.	-4.620×10^{-10}		-9.240×10^{-10}		-1.370×10^{-9}		-1.832×10^{-9}		-1.980×10^{-9}	
C_2 in ² /lb. ft. ²	2.264×10^{-15}		9.058×10^{-15}		1.990×10^{-14}		3.559×10^{-14}		4.159×10^{-14}	

Constant for Equation 55

Note: G = Surface temperature
 θ = Thermal gradient

TABLE 2

Calculated hydrostatic pressure, specific gravity and temperature for various depths using the equation of state for sea water and different thermal gradients.

CASE		1	2	3	4	5
Surface Temp. °F		68	68	68	68	68
Thermal gradient °F/100 ft.		0.5	1.0	1.5	2.0	2.2
Depth (ft.)						
0	PRESS. (PSI)	0	0	0	0	0
	G _w	1.030	1.030	1.030	1.030	1.030
	TEMP. (°F)	68	68	68	68	68
1000	PRESS. (PSI)	440	440	440	440	440
	G _w	1.038	1.038	1.038	1.037	1.037
	TEMP. (°F)	73	78	83	88	90
2000	PRESS. (PSI)	890	889	888	886	883
	G _w	1.046	1.044	1.042	1.040	1.039
	TEMP. (°F)	78	88	98	108	111
3000	PRESS. (PSI)	1340	1340	1338	1336	1327
	G _w	1.053	1.050	1.045	1.039	1.037
	TEMP. (°F)	83	98	113	128	133
4000	PRESS. (PSI)	1790	1789	1788	1779	1767
	G _w	1.060	1.053	1.045	1.035	1.032
	TEMP. (°F)	88	108	128	148	154
5000	PRESS. (PSI)	2247	2239	2238	2219	2207
	G _w	1.066	1.056	1.044	1.028	1.023
	TEMP. (°F)	93	118	143	168	176

TABLE 5 (Cont'd)

CASE		1	2	3	4	5
Surface Temp. °F		68	68	68	68	68
Thermal gradient °F/100 ft.		0.5	1.0	1.5	2.0	2.2
Depth (ft.)						
6000	PRESS. (PSI)	2707	2689	2688	2659	2644
	G_w	1.072	1.057	1.040	1.019	1.011
	TEMP. (°F)	98	128	158	188	198
7000	PRESS. (PSI)	3167	3139	3131	3092	3074
	G_w	1.077	1.058	1.035	1.006	.996
	TEMP. (°F)	103	139	173	208	219
8000	PRESS. (PSI)	3627	3589	3571	3521	3496
	G_w	1.081	1.057	1.027	.992	.979
	TEMP. (°F)	108	149	188	228	241
9000	PRESS. (PSI)	4089	4039	4011	3941	3911
	G_w	1.085	1.055	1.018	.975	.960
	TEMP. (°F)	113	159	202	248	262
10,000	PRESS. (PSI)	4559	4489	4444	4354	4317
	G_w	1.089	1.052	1.008	.956	.938
	TEMP. (°F)	118	169	217	268	284

G_w = Specific gravity of Sea water at shown pressure and temperature as computed by Eq. 55.

The hydrostatic pressure u_H can also be rewritten as

$$u_H = \gamma_0 z + u_d \dots \dots \dots \text{Eq. 57}$$

- where
- u_H = hydrostatic pressure for sea water that takes into consideration the effect of the thermal gradient,
 - γ_0 = unit weight of pure water at standard conditions which is 4°C and atmospheric pressure at -62.4 lbs/cu ft,
 - z = depth,
- and
- u_d = deviation in hydrostatic pressure caused by considering the effect of the thermal gradient from the hydrostatic pressure calculated by assuming the unit weight of water is a constant.

Figure 18 shows a plot of the deviation in pressure u_d as a function of depth for different cases. With a thermal gradient of 0.5°F per 100 ft the deviation is about 225 psi at 10,000 ft depth or about 6 percent of the pressure calculated by multiplying the depth times the unit weight of water at standard conditions. Figure 19 is a plot of the specific gravity of sea water as a function of depth for different cases. It shows that the deviation in specific gravity can be as much as 8% at 10,000 ft with a thermal gradient of 0.5°F per 100 ft.

All preliminary thermal data for the marine sediments show that the thermal conductivity increases as the porosity decreases. Therefore the thermal gradient should not be a constant except in constant porosity formations if the heat flux vector is constant with respect to depth, i.e., there are no local heat sources.

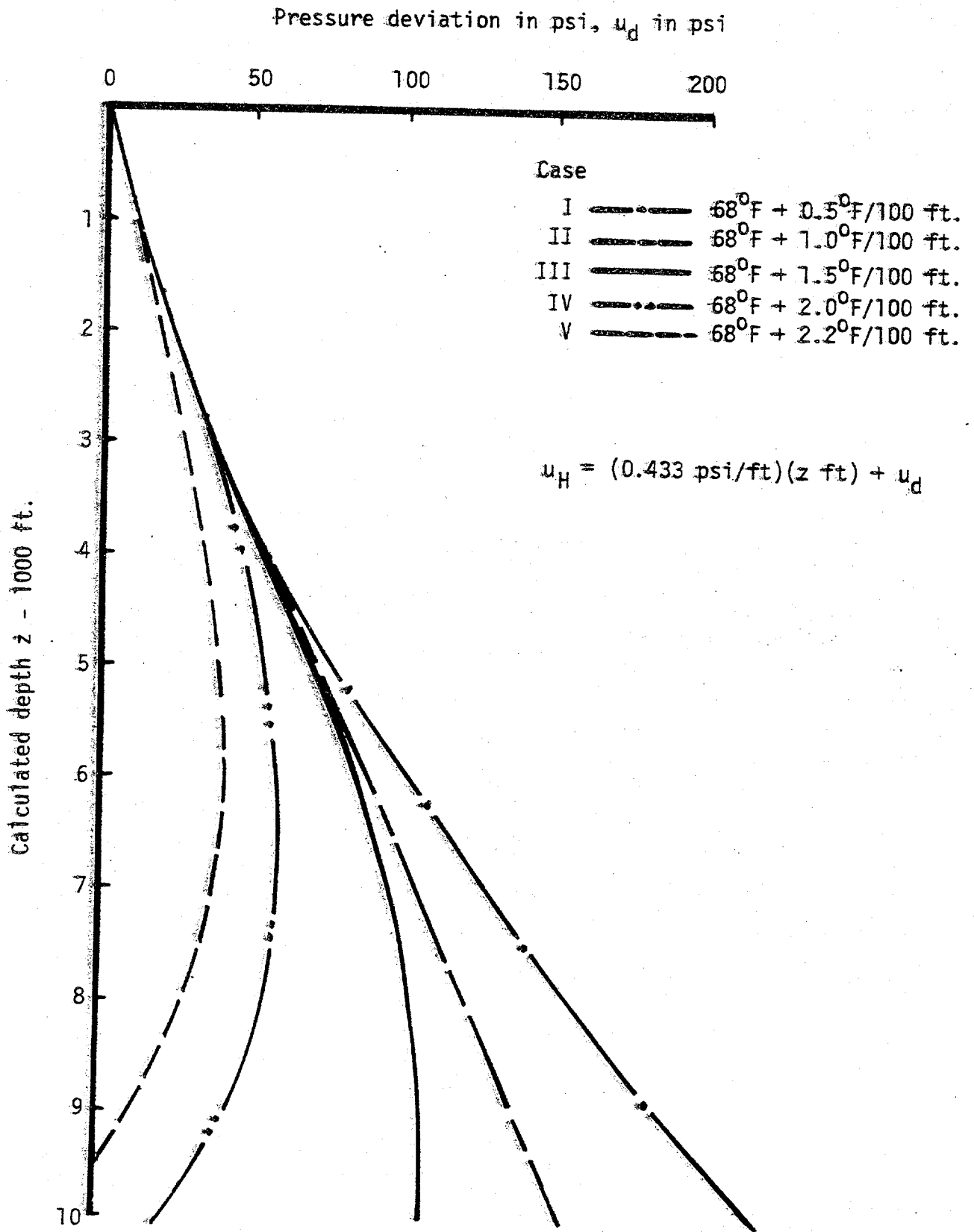


FIG. 18 - Deviation of calculated hydrostatic pressure calculated by taking into consideration the effect of the thermal gradient and hydrostatic pressure calculated by assuming the specific gravity of water is one.

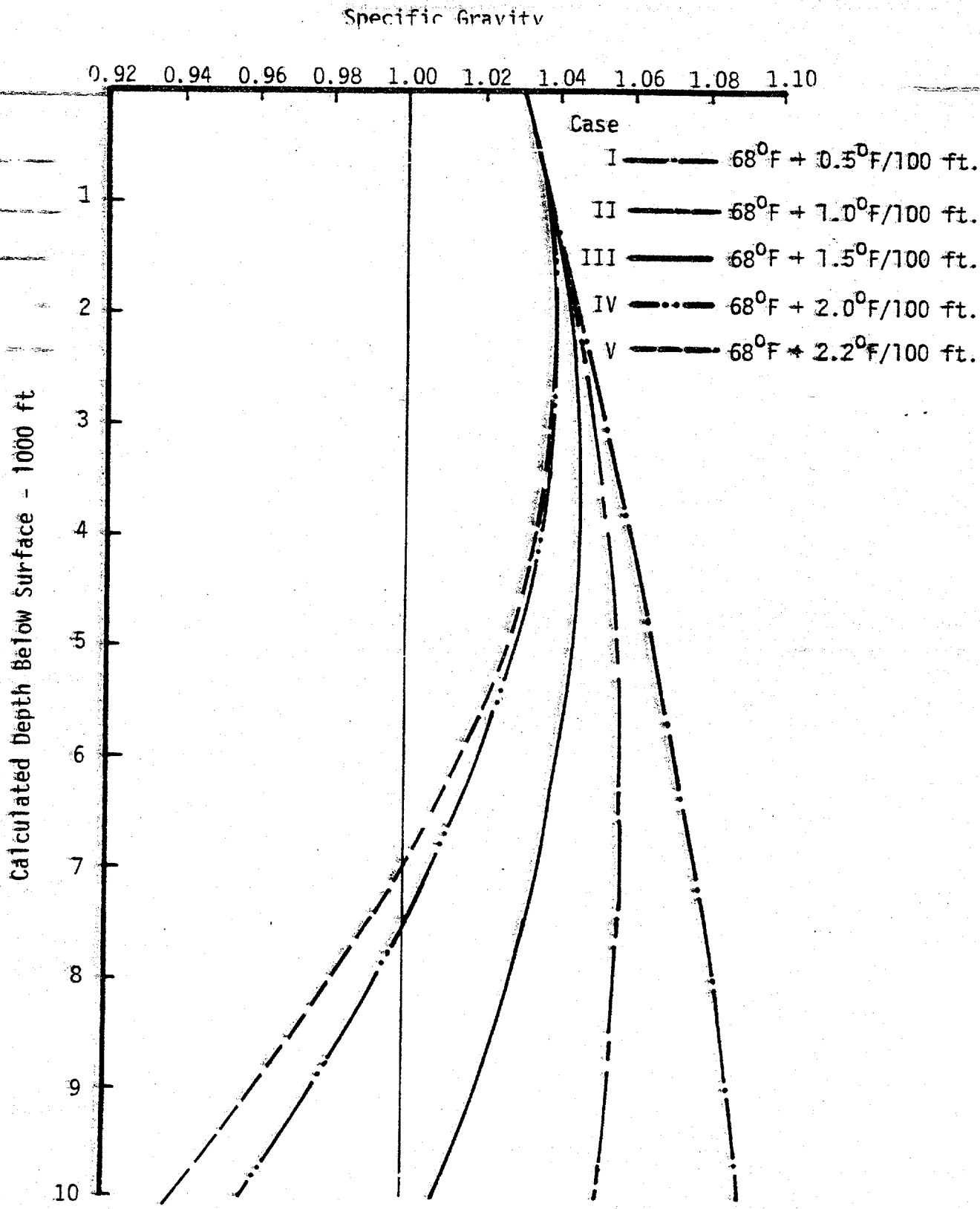


FIGURE 19 - Specific Gravity of Sea Water Hydrostatically Compressed with Different Thermal Gradients

8. POROSITY - DEPTH RELATIONSHIP FOR NORMALLY CONSOLIDATED FORMATIONS AT CONSTANT TEMPERATURES

The porosity-depth relationship can be computed for a normally pressured formation if it is assumed the density of the pore water is a constant.

The total stress σ is equal to the weight of the overburden of the depth Z distributed over a total unit area

$$\sigma = \int_0^Z \gamma_T dz \dots \dots \dots \text{Eq. 6}$$

where the total unit weight γ_T can be written as a function of the porosity n , as

$$\gamma_T = (1 - n)(G_S)(\gamma_0) + \gamma_0 G_W n \dots \dots \dots \text{Eq. 58}$$

where n = porosity

γ_0 = unit weight of water at the standard reference temperature and pressure.

G_S = specific gravity of the mineral solids.

G_W = specific gravity of the salt water - 1.03.

As shown before equilibrium requires

$$\sigma = \sigma' (1 - n^E) + un^E \dots \dots \dots \text{Eq. 5}$$

where σ' = mineral stress

u = pore pressure

σ = total stress

and n = porosity

$E \approx 1$ for a clay or shale

As shown before, the compressibility of the sediment may be represented by a power law so that

$$\sigma = \gamma_0 G_w z = +An^B \quad \dots \dots \dots \text{Eq. 70}$$

where A and B are compressibility constants for a given sediment.

If it is assumed that the pore pressure is equal to the hydrostatic stress and the specific gravity of water is a constant then

$$u = \gamma_0 G_w z \quad \dots \dots \dots \text{Eq. 59}$$

Combining all of the above equations produces

$$An^B + \gamma_0 G_w z n = \int_0^z \{(1-n)(G_s) \gamma_0 + n G_s \gamma_0\} dz$$

$$An^{B-1} + \gamma_0 G_w z = \int_0^z \left\{ \left(\frac{1-n}{n} \right) G_s \gamma_0 + G_s \gamma_0 \right\} dz$$

$$A(B-1)n^{B-2} \frac{dn}{dz} + \gamma_0 G_w = \left(\frac{1-n}{n} \right) G_s \gamma_0 + G_s \gamma_0$$

$$\frac{A(B-1)n^{B-1}}{G_s \gamma_0 (1-n)} dn = dz \quad \dots \dots \dots \text{Eq. 60}$$

to obtain finally the following integral.

$$z = \frac{A(B-1)}{G_s \gamma_0} \int_{n=n_0}^{n=n_z} \frac{n^{B-1}}{1-n} dn \quad \dots \dots \dots \text{Eq. 61}$$

The terms in front of the integral sign are all constants for a given clay or shale.

$$\gamma_0 = 1 \text{ gm/cc} = 62.4 \text{ lbs. per cu. ft.}$$

$$G_s \approx 2.74 \text{ for the usual clay minerals}$$

$$0 < A < 3 \text{ for the usual sediments tested}$$

$$-11.21 < B < -5 \text{ for the usual sediments tested}$$

B = - 23.55 for Ottawa sand.

It should be noted that A & B are not necessarily integers and that B is always negative. Since

$$\frac{1}{1-n} = \sum_{m=0}^{\infty} n^m \dots \dots \dots \text{Eq. 62}$$

the integral can be rewritten as

$$z = \frac{A(B-1)}{G_s \gamma_0} \int_{n=n_0}^{n=n_z} (n^{B-1} \sum_{m=0}^{\infty} n^m) dn \dots \dots \dots \text{Eq. 63}$$

This can be integrated term by term to yield

$$z = \frac{A(B-1)}{G_s \gamma_0} \left\{ \sum_{m=0}^{\infty} \frac{n^{B+m}}{B+m} \right\} \Big|_{n=n_0}^n \dots \dots \dots \text{Eq. 64}$$

or when the limits are taken where n_0 is the porosity at the ocean bottom and about equal to 0.85 and n is the porosity at depth z .

$$z = \frac{A(B-1)}{(G_s)(\gamma_0)} \left\{ \sum_{m=0}^{\infty} \frac{n^{B+m}}{B+m} - \sum_{m=0}^{\infty} \frac{n_0^{B+m}}{B+m} \right\} \dots \dots \dots \text{Eq. 65}$$

Since n is always less than one there will be very little contribution to the solution of any term when $B+m > 1$ but there will be a large contribution when $B+m < 1$.

Therefore the number of terms needed for convergence is $m = -B$ because B is always negative.

Table 6 gives the normal pressured formation depth-porosity relationship for the sediments tested and Figure 20 shows a plot of these results.

TABLE 6 . Calculated Porosity Ratio Depth Relationship for Different Sediments with Hydrostatic Constant Temperature Pore Water Stress.

Type of Sediment	Virginia	Miss. Delta	Campeche	Hawaii	South China	Ottawa Sand
A*	1.8	0.35	2.73	5.39	0.37	7.4×10^{-8}
B*	-5.5	-11.21	-6.13	-5.71	-10.1	-23.55
Porosity Ratio	Calculated Depth in Feet					
0.85	0.0	0.0	0.0	0.0	0.0	0.0
0.8	9.80	10.87	18.41	19.84	7.94	0.0001
0.75	21.32	29.11	40.94	43.48	20.41	0.0002
0.7	35.90	63.06	70.68	73.81	41.92	0.0011
0.65	55.56	132.18	112.63	115.34	82.34	0.0052
0.6	83.71	286.49	175.72	175.78	165.08	0.0294
0.55	126.76	666.32	276.87	269.32	350.5	0.1997
0.5	195.89	1,708.73	450.60	423.9	809.74	1.6758
0.45	316.67	4,952.37	772.99	698.79	2,085.66	18.04
0.4	545.13	16,677.85	1,427.73	1,231.21	6,150.20	262.98
0.35	1,022.95	67,693.18	2,911.62	2,374.96	21,475.43	5,599.61
0.3	2,157.44	-----	6,775.72	5,175.37	93,187.87	-----
0.25	5,344.16	-----	18,876.84	13,331.85	-----	-----
0.2	16,690.16	-----	68,064.56	43,681.62	-----	-----
0.15	74,890.75	-----	-----	-----	-----	-----
0.1	-----	-----	-----	-----	-----	-----

* Compressibility Factors in Equation 10.

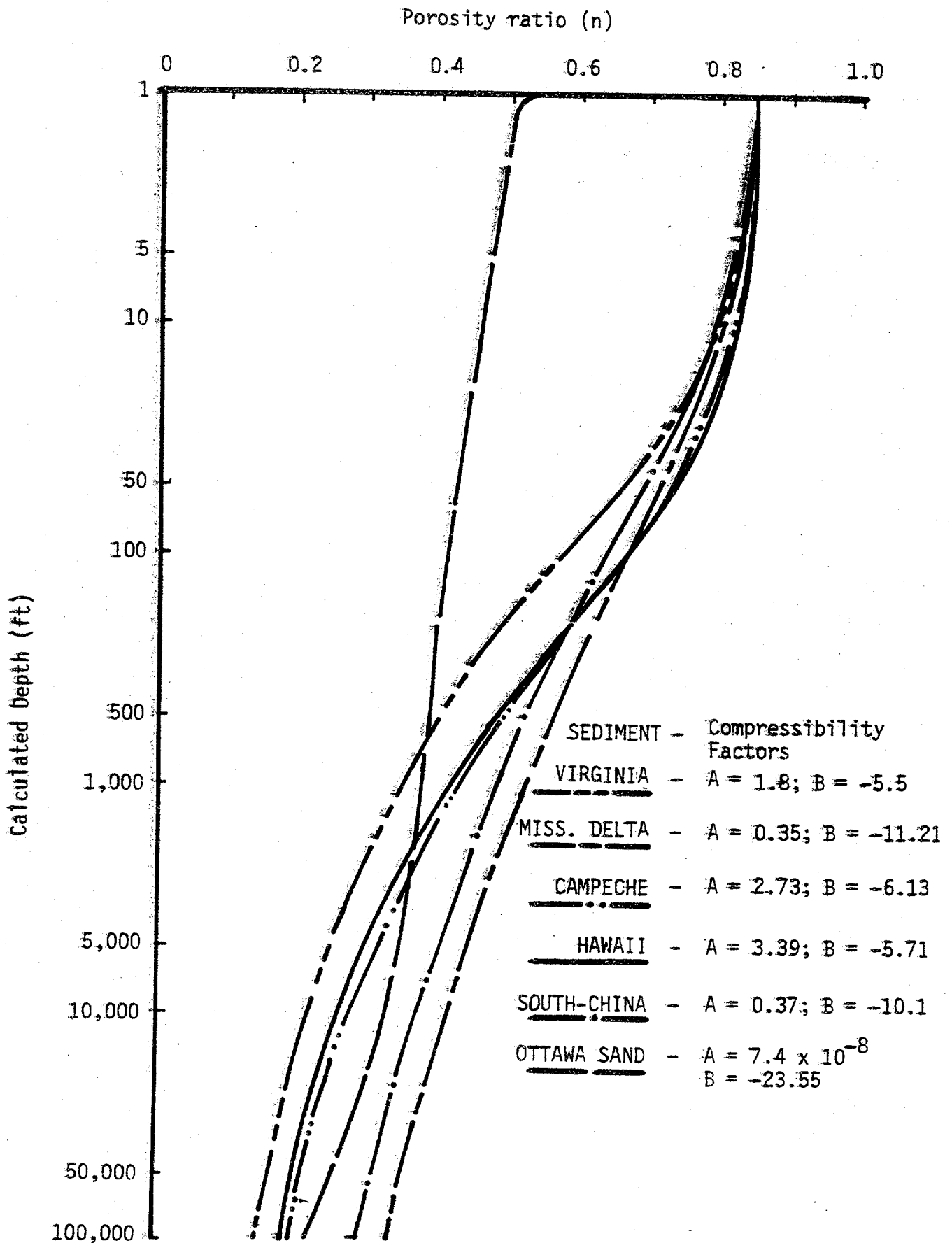


FIGURE 20 - Plot of Computed Porosity Ratio Depth Relationship - With Hydrostatic Pore Stress at Constant Temperature.

If the porosity is measured at a depth and it is larger than the value computed then the material is underconsolidated and overpressured. The percent consolidation U can be computed as follows. Calling the above calculated porosity n_c , and the porosity at the ocean bottom n_0 , which is the maximum porosity and the measured porosity n_z at depth z then

$$U = \frac{n_0 - n_z}{n_0 - n_c} \dots \dots \dots \text{Eq. 66}$$

It is interesting to note the same type of equation for the porosity-depth is produced if the Terzaghi effective stress concept is used instead of the effective force concept. In this case $\bar{\sigma}$ is the effective stress and

$$\sigma = \bar{\sigma} + u \dots \dots \dots \text{Eq. 67}$$

taking $\bar{\sigma} = An^B$ from the experimental test results then

$$An^B + \gamma_0 G_w z = \int_0^z \{(1-n)G_s \gamma_0 + n G_w \gamma_0\} dz$$

$$A(B-1)n^{B-1} \frac{dn}{dz} + \gamma_0 G_w = (1-n) G_s \gamma_0 + n G_w \gamma_0$$

$$A(B-1)n^{B-1} \frac{dn}{dz} = (1-n)G_s \gamma_0 - (1-n) G_w \gamma_0$$

$$A(B-1)n^{B-1} \frac{dn}{dz} = (1-n)(\gamma_0)(G_s - G_w) \dots \dots \dots \text{Eq. 68}$$

$$z = \frac{A(B-1)}{\gamma_0(G_s - G_w)} \int_{n=n_0}^{n=n_z} \frac{n^{B-1}}{1-n} dn \dots \dots \dots \text{Eq. 69}$$

The only difference between Equation 69 and Equation 61 is the constant in front of the integral. Comparing the two constants and taking $G_s = 2.70$ and $G_w = 1.03$ then the Terzaghi assumption requires that the depth for a given porosity

be 1.62 times the depth calculated using the mineral stress concept.

This difference may make it possible to test whether the effective stress or effective force concept is correct, or to evaluate the void area constant E for a given sediment type. Such a test would be a sedimentation experiment in the laboratory in which the porosity is measured as a function of depth after the sediment stops consolidating.

It is important to establish the effective force concept experimentally as well as theoretically so the drilling industry can prepare itself for hypergeostatic pressures if hypergeostatic pressures can occur in deep rock formations. In the past the effective stress concept has been accepted and there has even been a reluctance to report pressures that exceed the depth times 1 psi even though greater pressures may have been involved in many catastrophic blowouts. The assumed maximum total stress gradient of 1 psi per foot of depth requires that the average total unit weight of the material to be equal to 144 lbs/cu ft or that the average porosity ratio be about 0.26. Even if the pore pressure is hydrostatic none of the materials tested will compress under its own weight to an average porosity ratio of 0.26 in 50,000 ft. This is illustrated by the calculated porosity-depth curves in Fig. 20.

9. VARIATION IN PORE WATER PRESSURE
IN CONSTANT POROSITY FORMATIONS

In the petroleum industry it has been observed that the zones immediately overlying many highly overpressured formations are shales that have very little or no variation in porosity with respect to depth as shown in Figure 21. In some regions the porosity even increases with greater depth.

It is interesting to study the variation in pore pressure that can be expected when drilling into these "seal" formations so that the driller can "weight up" his drilling fluid in anticipation of penetrating a sand member that could cause a blowout.

Again equating the force in water plus the force in the mineral matrix to the overburden force it has been shown that

$$\sigma = An^B + un = \int_0^z \{(1-n) G_s \gamma_0 + nG_w \gamma_0\} dz \dots \dots \dots \text{Eq. 44}$$

By taking the derivative with respect to depth to remove the integral then

$$(ABn^{B-1} + u) \frac{\partial n}{\partial z} + n \frac{\partial u}{\partial z} = (1-n) G_s \gamma_0 + nG_w \gamma_0 \dots \dots \dots \text{Eq. 70}$$

If the porosity is constant in the formation then $\frac{\partial n}{\partial z} = 0$ and the equation becomes

$$\frac{\partial u}{\partial z} = \gamma_0 G_s \frac{(1-n)}{n} + G_w \gamma_0 \dots \dots \dots \text{Eq. 71}$$

or
$$u = z\gamma_0 \left\{ G_s \left(\frac{1-n}{n} \right) + G_w \right\} + H \dots \dots \dots \text{Eq. 72}$$

The first term of the right hand side of Equation 71 is the excess pore pressure gradient since the second term is the hydrostatic pressure gradient.

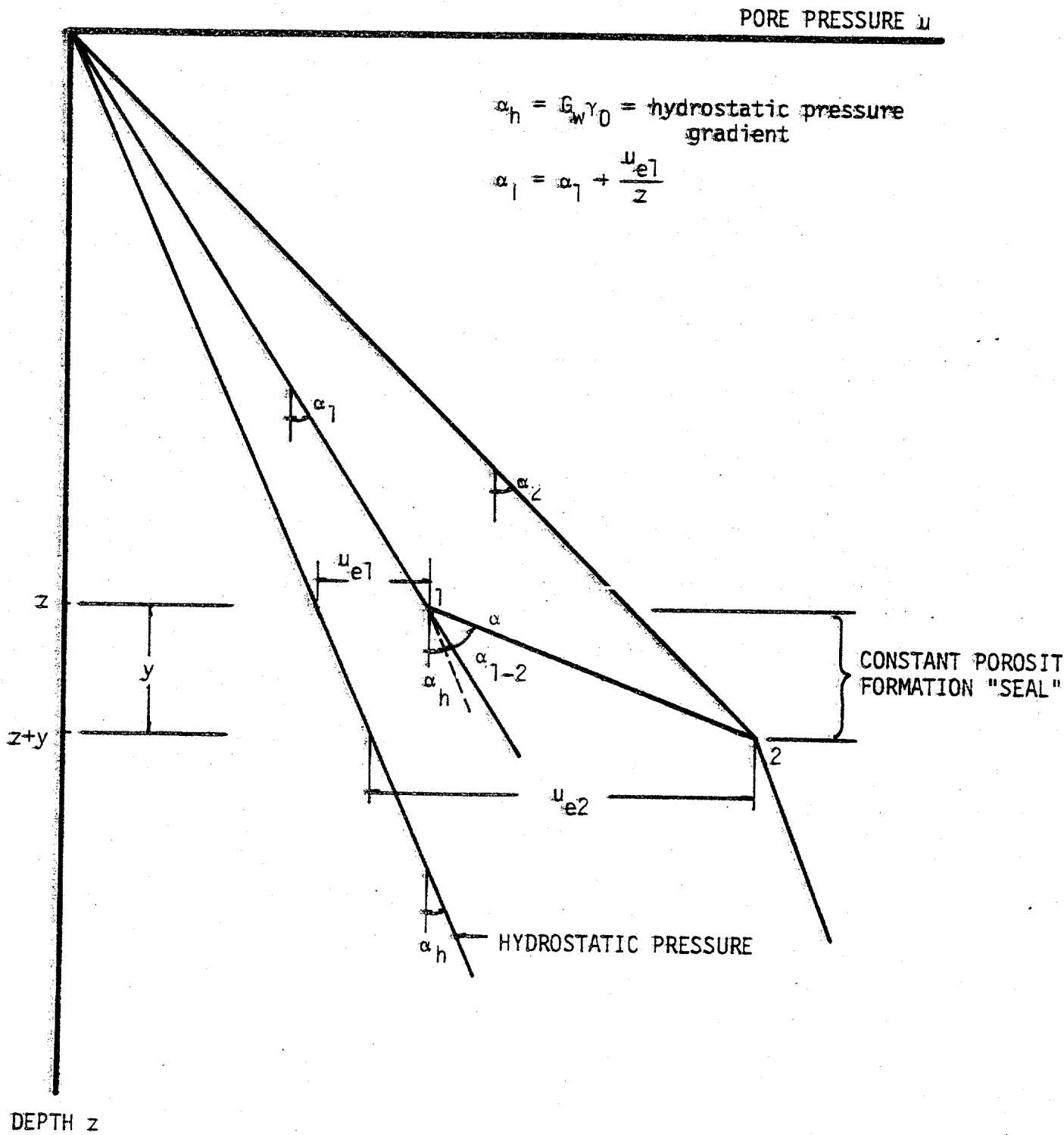


FIG. 21

CHANGE IN PRESSURE-DEPTH RATIO IN CONSTANT POROSITY FORMATION

As shown in Figure 21 the pressure-depth ratio α , at the top of the seal at point 1 is given by α_1 . It can be written as the sum of the hydrostatic and excess pore pressure divided by the depth. Therefore

$$\alpha_1 = \gamma_0 G_w + \frac{u_{e1}}{z} \dots \dots \dots \text{Eq. 73}$$

where u_{e1} = the excess pore pressure at point 1.

The pore pressure u_2 at point 2 can be computed as follows:

$$u_2 = \alpha_1 z + \left(\frac{\partial u}{\partial z}\right) y \dots \dots \dots \text{Eq. 74}$$

where y is the distance drilled into the seal, therefore

$$u_2 = \alpha_1 z + \left\{ \gamma_0 G_s \frac{(1-n)}{n} + G_w \gamma_0 \right\} y$$

but $\alpha_2 = \frac{u_2}{z+y}$

therefore

$$\alpha_2 = \frac{\alpha_1 z}{z+y} + \left\{ \frac{G_s(1-n)}{n} + G_w \right\} \frac{y\gamma_0}{z+y} \dots \dots \dots \text{Eq. 75}$$

For an example, if $\alpha_1 = 0.5$ psi/ft., $z = 10,000$ ft., $G_s = 2.7$, $G_w = 1.03$, $y = 100$ ft and $n = 0.67$ then

$$\alpha_2 = \frac{\alpha_1(10,000)}{(10,100)} + \left(2.7 \frac{(1-0.67)}{0.67} + 1.03 \right) \frac{(62.4)(100)}{(144)(10,100)}$$

$$\alpha_2 = (0.5)(0.99) + (2.36)(0.433)(0.0099)$$

$$\alpha_2 = 0.50512 \text{ psi/ft}$$

Therefore a mud weight of at least 9.72#/gal is needed in the borehole to equalize the formation pressure.

Had the constant porosity formation been 1000 ft thick then

$$\alpha_2 = (0.5)\left(\frac{10,000}{11,000}\right) + (2.36)(0.433)\left(\frac{1,000}{11,000}\right)$$

or
$$\alpha_2 = 0.4546 + 0.0929 = 0.54745 \text{ psi/ft}$$

Therefore, a mud weight of 10.53 #/gal is needed to equalize formation pore pressure.

Had the Terzaghi assumption been used where $\sigma = An^B + u$ then Equation 71 would have to be written as

$$\frac{du}{dz} = (1-n)(G_s)(\gamma_o) + nG_w\gamma_o \text{ Eq. 76}$$

or
$$u = z\gamma_o \{(1-n)(G_s) + n G_w\gamma_o\} \text{ Eq. 77}$$

The pore pressure gradient of Equation 76 can be obtained by multiplying pressure gradient of Equation 71 by the porosity ratio which is always less than one. For the first example α_2 would become 0.50183 psi/ft and in the second example α_2 would become 0.5168 psi/ft if the Terzaghi effective stress concept had been used instead of the effective force concept.

A little reflection will show that the computed pore pressure gradient of Equation 71 is the greatest that can exist in a constant porosity formation. The water must support any added overburden above the formation without a decrease in porosity. This maximum pore pressure gradient is the

slope of the pore pressure function not the pore pressure divided by the depth of the formation. As shown by Equation 71 it is the total unit weight of the formation divided by the porosity ratio.

10. EQUILIBRIUM REQUIREMENT FOR POREWATER
PRESSURE AT INTERFACES

The equilibrium condition can also be applied to the interface between two different formations and the total force must be the same in each if static equilibrium exists.

At the horizontal interface between shale and sandstone the pore pressure and the total stress in each must be the same. Using these requirements and Equation 10, then

$$u_s n_s^E s + A_s n_s^B s = u_c n_c^E c + A_c n_c^E c \dots \dots \dots \text{Eq. 78}$$

where all subscripts s denote the sand and all subscripts c denote the shale.

For the sand E_s is very small and $n_s^E s$ approaches 1; for the shale E_c is probably about 1 and $n_c^E c$ approaches n_c . Therefore

$$u + A_s n_s^B s = u n_c + A_c n_c^B c \dots \dots \dots \text{Eq. 79}$$

Solving for u gives

$$u = \frac{A_c n_c^B c - A_s n_s^B s}{1 - n_c} \dots \dots \dots \text{Eq. 80}$$

This expression shows that unless the materials have been unloaded the pore pressure is not independent of the porosity of the two different formations.

For a water to horizontal rock or sediment interface, the same

requirements produce

$$u = un^E + An^B \quad \dots \dots \dots \text{Eq. 81}$$

solving for u gives

$$u = \frac{An^B}{1-n^E} \quad \dots \dots \dots \text{Eq. 82}$$

This expression shows that the porosity of a sediment on the ocean bottom is not independent of the depth of the water. However, laboratory tests have shown that the porosity ratio n falls in the range of $n = 0.80$ to 0.85 for several different sediments when $u = 0$.

The same principle can be used to compute the drilling fluid pressure (mud slurry) u_m required to balance the vertical sand formation force.

Using Equation 6 then

$$u_m = un_s^{E_s} + A_s n_s^{B_s} \quad \dots \dots \dots \text{Eq. 83}$$

where u = formation water pore pressure,

n_s = formation (sand) porosity,

E_s = area power law constant for sand (very small ~ 0.09) so

that $n_s^{E_s} \approx 1$

and A_s and B_s are the compressibility factors for sand.

At each of the interfaces considered, it has been assumed that the forces on either side of the interface are in equilibrium. It has also been assumed that the force in the fluid plus the force in the mineral matrix

are equal to the total force. This is in contrast to the Terzaghi effective stress principle that requires the stress in the fluid plus the effective stress to be equal to the total stress.

According to the Terzaghi effective stress principle the fluid stress is a neutral stress. It can alter the spherical stress only; it cannot produce shear stress or principle stress differences.

When this principle is applied to the interface along the side of a borehole where the pressure in the borehole fluid is higher than the pressure in the formation fluid, the only thing that will happen is that the fluid will flow from the borehole into the formation and the formation pressure will increase in the immediate vicinity of the well bore. According to Terzaghi's effective stress principle the borehole fluid cannot push against the sides of the borehole mineral matrix; it only changes the spherical stress.

This may be nearly true for a very porous highly permeable sand or gravel where the contact area between grains is very small; however, it is contrary to fact for sandstone, limestone, shale and other formations with lower porosities. The borehole fluid does exert force on the mineral matrix at the borehole interface; radial vertical cracks develop as the diameter of the borehole increases. This is the phenomena of hydrofracture(18).

It could be argued that the borehole fluid contains suspended clay particles that clog up the pores in the formation and form a "filter cake" in the formation. Now the borehole fluid could exert an internal pressure on an impermeable pipe and cause it to rupture.

Were this the case the cracks could only propagate the thickness of the "filter cake" and this is known not to be true. Also, it is very difficult to apply the "filter cake" reasoning to the borehole interface when the borehole fluid is either kerosene or varsol. There are no

suspended clay particles to form the filter cake. These are the usual borehole fluids used to expand the borehole and propagate radial cracks for many diameters of the well. This is standard oil field practice to increase the permeability of oil bearing formation (18). It is also physical evidence that Terzaghi's effective stress principle does not apply to formations with significant contact area between mineral particles.

11. THERMODYNAMICS OF PROGRESSIVE BURIAL OF SEDIMENT

It has been observed that many overpressured zones have high porosities and higher than normal thermal gradients. It has generally been assumed that these high porosity formations all have low thermal conductivities. Since the product of the thermal conductivity and the temperature gradient is equal to the heat flux, if Fourier's Law applies, it follows that the temperature gradient must increase when the thermal conductivity decreases if the heat flux is constant with respect to depth (22).

This reasoning implies that the overpressured formation is the cause of the high temperatures. Another group has theorized that the high temperature has caused the high pressures and the high pressures have preserved the high porosities (4).

It has been assumed that because of faulting, some formations have been dropped. If the thermal gradient remains the same and the dropped formation is covered or sealed with nearly impermeable clay or shale the water will be heated and if it cannot escape high pressures will result.

Each of these explanations assumes the thermodynamics is separate from the mechanics of progressive burial of sediment, when in reality they are coupled. In fact if the material is properly described by constitutive equations for stress, internal energy, entropy and heat flux, then the field equations (conservation laws) should make it possible to predict both temperature and motion as a function of space and time.

As a material is compressed the irrecoverable strain energy is converted into heat. That heat which does not escape through either conduction or convection must raise the temperature of the sediment and the water in it. This is called the heat of compaction.

There are two other sources of heat to be considered; the heat

generated by the decay of dispersed radioactive elements and the heat dissipated from the hot core of the earth as it cools.

The sum of these three heat flows has been indirectly measured in a great many places in the ocean bottom and in many continental locations (9). This is accomplished by measuring the temperature at two different depths several feet apart. If the thermal conductivity of the material is known the heat flux can be computed by Fourier's law.

The variation of thermal flux over the oceans is shown in Figure 22 (21). The variation in temperature with depth for several oil wells in Chocolate Bayou field, Brazoria County, Texas is shown in Figure 15 (6). Figure 16 gives the bottom hole pressure for these same wells in Brazoria County, Texas. Figure 17 presents contours of equal thermal gradient for the East Texas area. These are based on the bottom hole temperature and the depth of the well.

The heat of compaction holds the most interest because the dissipated mechanical energy is the source of the heat. This source develops only if there is drainage so that the sediment can compress. With compression comes bottom subsidence and a decrease in potential energy of the sediment. There is an increase in potential energy of the water.

As the sediment compresses its strain energy increases. However, only a part of the strain energy is recoverable. That which is irrecoverable is converted to heat. A part of this heat is conducted upward toward the surface and the other part of the heat is stored in the sediment and its interstitial water.

The increase in temperature will tend to lower the density and the increase in pressure will tend to increase the density. Any increase in water pressure increases the excess pore water pressure gradient which

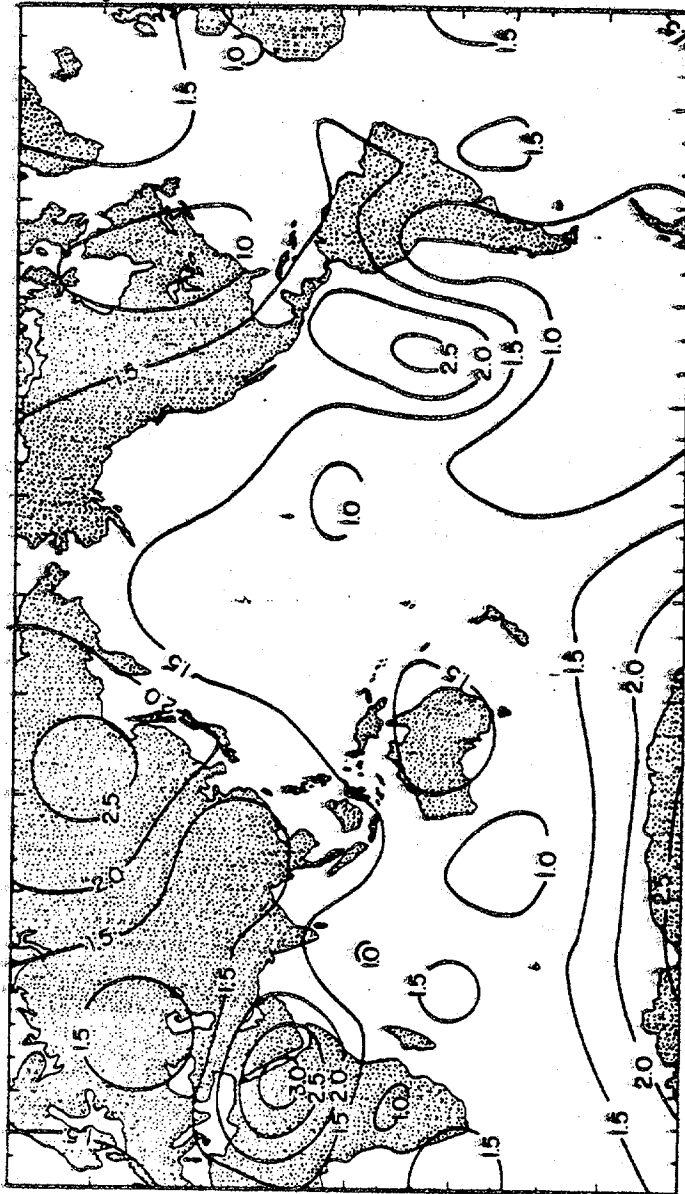


FIG. 22 - Contour map of heat flow, 10^{-6} cal/cm²-sec (21).

tends to cause water drainage. If drainage does occur the water pressure and temperature decreases.

As the sediment is compressed its permeability decreases also. For sediments with significant clay content, the permeability decreases orders of magnitude faster than the porosity, and strangulates the drainage.

If the water is prevented from draining, there is no subsidence and no irrecoverable strain energy for a heat source. As sediment is added at the mudline the weight of the added material is supported by both the mineral and the water. There will be a small increase in strain energy in the water. All of this energy is recoverable except the heat lost to conduction. The compressibility of individual clay particles can be ignored because it is thought that their compressibility is about one order of magnitude lower than the compressibility of water.

The field equations used thus far have included conservation of mass, linear momentum and moment of momentum. The interaction between the water and the mineral has been described by Darcy's law. The mineral matrix has been described by the compressibility and permeability functions. Temperature and energy have been ignored.

To account for the thermodynamics of progressive burial of sediment there remains the principle of conservation of energy, the entropy inequality, the specific heat concept and Fourier's heat conduction "law".

When the conservation of linear momentum, moment of momentum and mass equations are combined with the conservation of energy equation the reduced energy equation results (12). For the one-dimensional case with both uniaxial compression and heat flow the reduced energy equation becomes

$$p \dot{\xi} = \sigma \dot{\epsilon} + \frac{\partial h}{\partial z} + \rho s \quad \dots \dots \dots \text{Eq. 84}$$

- where
- $\dot{\xi}$ = rate of change of internal energy per unit mass,
 - γ = mass density,
 - σ = vertical stress on a horizontal plane,
 - h = heat flux vector out of the material where $-h$ points in the direction energy is flowing through the boundary,
 - s = the supply or source of heat-decay of dispersed radioactive minerals,
 - z = the depth which is positive downward,
 - $\dot{\epsilon}$ = rate of change of strain where for the mineral,
 - $\dot{\epsilon} = \frac{\partial n}{\partial t}$ = rate of change of porosity.

The reduced energy equation can be applied to the mineral or the water individually or to them collectively.

The first term on the right hand side of Equation 84 is called the Stokes working or the stress power. It is the rate of change of strain energy put into the material. The second term on the right hand side of Equation 84 is the divergence of the heat flux vector. The third term is the local supply of heat. The sum of the last two terms is called the local heating. The heat flux vector, h , includes the heat of compaction, the heat generated by the decay of radioactive minerals, and the heat from the molten core of the earth conducted upward through the crust.

The internal energy (12) does not include the potential or gravitation energy but it does include the recoverable strain energy and the thermal energy. The internal energy description is but one of the group of material description equations needed to solve a thermomechanical problem. The other

material description equations (constitutive equations) are for the stresses, heat flux and entropy. If these equations are objective they must be functions of the strains, strain rates and temperature. When the proper constitutive equations are combined with the conservation or field equations, theoretically it is possible to uniquely predict motion and temperature changes. Only by comparing measured motions and temperature changes with predicted values can a theory or material description be substantiated. This is because the only things that can be measured are relative motions and temperature changes (32).

Taking the first constitutive equation for the uniaxial problem as

$$\rho \dot{\xi} = C_{V\rho} \dot{\theta} + \sigma \dot{\epsilon}_r \quad \text{Eq. 85}$$

where $C_{V\rho}$ = specific heat of the material at a constant volume times the mass density.

θ = rate of change of temperature

σ = vertical stress on the horizontal plane

ϵ_r = rate of change of recoverable energy or the recoverable working.

The first term on the right hand side of Equation 85 is the rate of change of thermal energy as given by the specific heat concept and the second term is the recoverable working or rate of change of recoverable strain energy. This equation can be applied to the mineral or to the water individually or to them collectively.

It should be noted that all stresses are recoverable; it is the strains that can be divided into recoverable and irrecoverable components.

When Equation 84 and Equation 85 are applied to a unit volume of

mineral-sea water mixture with a porosity ratio of n then

$$\begin{aligned}
 & (1-n) \sigma' \dot{\epsilon} + n u \dot{\epsilon}_w + (1-n) \frac{\partial h_s}{\partial z} + n \frac{\partial h_w}{\partial z} + \rho_s s_s + \rho_w s_w \\
 & = (1-n) \sigma' \dot{\epsilon}_r + n u \dot{\epsilon}_{wr} + (\rho_w C_{vw} + \rho_s C_{vs}) \dot{\theta} \dots \dots \dots \text{Eq. 86}
 \end{aligned}$$

- where
- σ' = the stress in the mineral,
 - $\dot{\epsilon}$ = the input rate of strain of the mineral,
 - $\dot{\epsilon}_r$ = the recoverable rate of strain of the mineral,
 - u = the water pressure,
 - $\dot{\epsilon}_w$ = the input rate of strain of the sea water,
 - $\dot{\epsilon}_{wr}$ = the recoverable rate of strain of the sea water,
 - h_s = the heat flux through the mineral only in a unit volume of the mixture,
 - h_w = the heat flux through the sea water only in a unit volume of the mixture,
 - $\rho_s s_s$ = the heat supply rate in the mineral only in a unit volume of the mixture,
 - $\rho_w s_w$ = the heat supply rate in the sea water only in a unit volume of the mixture,
 - $\rho_s C_{vs}$ = specific heat of the mineral only in a unit volume of the mineral-sea water mixture,
 - $\rho_w C_{vw}$ = specific heat of the sea water only in a unit volume of the mineral-sea water mixture,
 - $\dot{\theta}$ = rate of change of temperature.

If it is assumed that the water strain ϵ_w is equal to the recoverable water strain, ϵ_{wr} , then Equation 86 can be rewritten as

$$\begin{aligned}
(1-n) \sigma' (\dot{\epsilon} - \dot{\epsilon}_r) &= (\rho_w C_{vw} + \rho_s C_{vs}) \dot{\theta} \\
- \left\{ (1-n) \frac{\partial h_s}{\partial z} + n \frac{\partial h_w}{\partial z} \right\} \\
- \{ \rho_w s_w + \rho_s s_s \} & \dots \dots \dots \text{Eq. 87}
\end{aligned}$$

The constitutive equation for stress can be taken from Equation 10 which is

$$\sigma' = \frac{An^B}{1+n^E} - c \dots \dots \dots \text{Eq. 88}$$

This same equation was used in the calculation for the rate of dissipation, Equation 20, therefore, if $E = 1$ for shales or clays then,

$$\begin{aligned}
(1-n) \sigma' (\dot{\epsilon} - \dot{\epsilon}_r) \\
= An^B \left[1 - (10A)^{-B-1} (1-B B_u^{-1}) n^{(-B B_u^{-1})} \right] \frac{\partial n}{\partial t} \dots \dots \text{Eq. 89}
\end{aligned}$$

The Clausius-Planck principle requires that the rate of dissipation always be zero or positive. Equation 89 is equivalent to an equation for the rate of change of entropy (34). From Equation 31

$$\rho_w C_{vw} + \rho_s C_{vs} = n G_w \gamma_0 C_{vw} + (1-n) G_s \gamma_0 C_{vs}$$

the supply terms can be written as

$$\rho_w s_w + \rho_s s_s = n G_w \gamma_0 s_w + n G_s \gamma_0 s_s \dots \dots \dots \text{Eq. 90}$$

The total heat flux h_T through both mineral and sea water can be defined as

$$\frac{\partial h_T}{\partial z} = (1-n) \frac{\partial h_s}{\partial z} + n \frac{\partial h_w}{\partial z} \dots \dots \dots \text{Eq. 91}$$

The last constitutive equation can be obtained by assuming the Fourier heat conduction "law" applies, then

$$h_T = k_h \frac{\partial \theta}{\partial z} \dots \dots \dots \text{Eq. 92}$$

therefore

$$\frac{\partial h_T}{\partial z} = k_h \frac{\partial^2 \theta}{\partial z^2} + \frac{\partial \theta}{\partial z} \left(\frac{\partial k_h}{\partial z} \right) \dots \dots \dots \text{Eq. 93}$$

From Equation 30 as determined by tests

$$k_h = E + Fn + Gn^2$$

therefore

$$\frac{\partial k_h}{\partial z} = (F + 2Gn) \frac{\partial n}{\partial z} \dots \dots \dots \text{Eq. 94}$$

Substituting these into Equation 91 yields

$$\frac{\partial h_T}{\partial z} = (E + Fn + Gn^2) \frac{\partial^2 \theta}{\partial z^2} \dots \dots \dots \text{Eq. 95}$$

if it is assumed that the product of differentials are small and can be ignored.

Combining Equations 89, 31, 90, 91, and 95 with Equation 87 produces

$$\begin{aligned}
 & A n^B \left[1 - (10A)^{-B-1} (1 - B B_u^{-1}) n^{(-B B_u^{-1})} \right] \frac{\partial n}{\partial t} \\
 & = \{ n G_w \gamma_o C_{vw} + (1-n) G_s \gamma_o C_{vs} \} \frac{\partial \theta}{\partial t} \\
 & - (E + F n + G n^2) \frac{\partial^2 \theta}{\partial z^2} \\
 & - \{ n G_w \gamma_o s_w + (1-n) G_s \gamma_o s_s \} \dots \dots \dots \text{Eq. 96}
 \end{aligned}$$

This is the energy equation for the progressive burial of sediment. It is a second order nonlinear partial differential equation with two dependent variables, temperature and porosity ratio n , and two independent variables, depth z and time t . The material coefficients A , B , and B_u as well as G_w and G_s all depend on temperature. The values of E , F , G , C_{vw} , C_{vs} , s_w and s_s may also depend on temperature to some extent. Equation 96 shows the coupling of the temperature and porosity ratio as the sediment consolidates and subsides.

At first glance it may seem highly doubtful that Equation 96 could have a unique solution, however, the porosity ratio must also satisfy Equation 50 which does have a unique solution. It is the simultaneous solution of both Equation 96 and Equation 50 that describes the porosity ratio and the temperature as functions of depth and time.

A cursory appraisal of Equation 96 shows that when the porosity ratio

n is a constant and the local heat supply is zero, Equation 96 will collapse into the familiar heat equation. It has a unique solution (3). If the temperature is a linear function of depth only and there is no local heat supply, then Equation 96 shows that the porosity ratio must be a function of depth only. If the porosity ratio n is a function of depth only, all consolidation and subsidence has ceased. In essence Equation 96 shows that consolidation produces heat and heat production causes the temperature to be generally a nonlinear function of depth and time.

12. A PRACTICAL APPLICATION OF RESEARCH; ESTIMATION OF PORE WATER PRESSURE WHILE DRILLING

Usually the first warning of an impending blowout or "kick" is a gain of volume of drilling fluid. Also, there is usually an increase in the drilling rate. Also, there is usually a decrease in mud pump pressure and an increase in mud pump speed. If the bulk density of the clay cuttings is monitored and it is found that the bulk density is not increasing and that the drilling rate has increased then the drilling fluid density can be increased in preparation for possible sand strata penetration. If drilling is stopped and well logs obtained the overpressured shales can be better recognized by no decrease to some increase in porosity with depth and a higher than normal temperature gradient. However, it is expensive to stop drilling to obtain well logs and even when overpressured shales are recognized the driller still does not know what drilling fluid density will be required for safe penetration of the sand formations. The methods now in use to detect overpressure zones are listed in Table 7 (14). The general description of overpressured rock formations is shown in Figure 1.

The drilling fluid is routinely screened through a "shale shaker" (vibrating screen) as it is returned to the "mud pit" from the well bore. The shale cuttings ordinarily are about 1/8" x 1/8" x 1/4" in size. The cuttings are removed primarily to preserve the drilling fluid properties, but they are also used to determine the formation porosity and mineralogical content. The porosity is measured by dropping them into a previously calibrated variable density fluid. They float at the depth at which their bulk specific gravity is the same as the specific gravity of variable density fluid (5), (1), (29).

TABLE 7. - Techniques used to detect overpressure in deeply buried rock formations (14)

Source of Data	Geophysical Method	Drilling Parameters	Drill Cuttings	Drilling Mud	Well Logging					
Parameters	"Formation" velocity (Seismic) Gravity Magnetics Electrical prospecting methods	Drilling rate "d" - Exponent Modified "d" - Exponent Drilling rate equations Torque Drag Drilling porosity log	Shale cuttings bulk density shale factor Electrical resistivity Volume Shape and size Novel geo-chemical and physical techniques	Gas content Flow line mud weight "Kicks" Flow line temperature Chlorine variation Drill pipe pressure technique Pit level and volume Flow rate Hole fill up Novel chemical and physical methods	Electrical surveys resistivity and conductivity Shale formation factor Salinity variations Internal transit time Bulk density Hydrogen index Thermal neutron capture cross section Nuclear magnetic resonance Downhole gravity data					
						Time of Recording	Prior to spudding well	While drilling	While drilling Delayed by the time required for mud return	After drilling

It seems from the work of Skempton (3) and this research that the compressibility factors A , B , and B_u can be related to the Atterberg limits of the sediment. The Atterberg limits are simple tests that can be run on the cuttings fairly quickly.

Equation 28 relates the recovered porosity ratio and the compressibility factors A , B , and B_u to the minimum pore water pressure of a formation. Therefore, it seems that the measured properties of the cuttings may make it possible to estimate the minimum pore water pressure of a formation while drilling.

The pore pressure in an interbedded sand formation will have to be less than the computed clay pore pressure. Since sand formations are relatively incompressible it is possible to estimate or guess the compressibility factors of a sand formation that might be encountered. With the total overburden force known it is then possible to estimate the porosity of the sand. Using the interface relationship between shale and water it is possible to get a better estimate of the pore pressure in the sand which will be lower than the clay pore pressure if there is drainage from the clay to the sand. This is shown by Equation 79.

Figure 20 shows the relationship between the porosity and depth for a normally consolidated clay or shale. If the cuttings indicate that the porosity is higher than this value then the driller can immediately be warned and the necessary tests made as outlined above to estimate the formation pore pressure. After this is done the driller can start his procedure to "weight up" his drilling fluid. Dave Powley of Amoco Oil Co. has noted that all of these calculations could be done readily on a preprogrammed mini-computer for use by site personnel.

13. CONCLUSIONS AND RECOMMENDATIONS

The study has been concerned only with the thermomechanical process of progressive burial of submarine sediment. Without doubt, there are other processes involved that are intrinsically related to the thermomechanical process that should be considered in future studies. In particular the cementation of the mineral matrix and the chemical action that alters the area of contact and the stiffness of the system should receive further study. However, this is the first step necessary for a mathematical analysis that shows how sediment responds to both heat and pressure as it is progressively buried.

Using the simplifying concept of vertical uniaxial strain and one dimensional vertical heat and water flow, the controlling differential equations for the progressive burial of sediment have been derived by returning to the classical field equations of continuum mechanics.

The field equations satisfied are for the conservation of mass, momenta, moment of momenta and energy. The entropy inequality is also satisfied. All of the field equations were applied to both the mineral and the interstitial water individually and collectively. The interaction between the mineral matrix and the interstitial water was described by Darcy's law. High pressure tests show that the coefficient of permeability can be described by a parabolic function of the porosity ratio.

A complete set of constitutive equations has been postulated to describe the materials. High pressure laboratory tests show that these equations fit the data nicely. The constitutive equations describe stress, rate of strain energy dissipation, rate of change of internal energy and the heat flux as functions of strain, rate of strain, temperature, temperature gradient and

rate of change of temperature. The vertical strain is equivalent to a change in porosity. The axioms of constitutive theory satisfied are for causality, determinism, equipresence, objectivity, material invariance, neighborhood, memory and admissibility.

The solution of the two controlling differential equations, consolidation and energy, will give the porosity ratio and temperature as a function of depth and time. These are measurable quantities; therefore, the theory is testable. Failure theory is nowhere involved.

Even though the controlling differential equations were derived for the uniaxial case, there seems to be no reason why the same ideas can not be extended to three dimensions. For instance, the constitutive equation for the total stress was written as

$$\sigma = (\sigma' + c) (1 - n^E) + un^E \quad \text{Eq. (5)}$$

where

$$(\sigma' + c) (1 - n^E) = An^B \quad \text{Eq. (10)}$$

and

$$u = f(G_w, \theta) \quad \text{Eq. (54)}$$

This equation can be extended to three dimensions by writing

$$\sigma_{ij} = (\sigma'_{ij} + c_{ij}) (1 - n^{E_{ij}}) + u_{ij} n^{E_{ij}} \quad \text{Eq. (97)}$$

$$(\sigma'_{ij} + c_{ij}) (1 - n^{E_{ij}}) = A_{ij} n^{B_{ij}} \quad \text{Eq. (98)}$$

where scalar quantities have been rewritten as tensor quantities. The scalar for total stress σ has become the stress tensor σ_{ij} , etc. Each of the scalar material descriptors A, B, E , etc. have become tensor descriptors A_{ij}, B_{ij}, E_{ij} , etc. where $i = 1, 2, 3$ and $j = 1, 2, 3$. The subscripts denote the

cardinal directions and as an example σ_{12} is the stress on plane perpendicular to the "1" direction acting in the "2" direction. Each tensor has nine components. A similar expression can be written for rate of strain energy dissipation, rate of change of internal energy and for the heat flux.

In particular it has been shown that equilibrium does not require that pore pressure be less than the geostatic stress. Using a new equation of state for sea water and assuming a linear thermal gradient, it has been shown that temperature and depth has a significant effect on hydrostatic pressure. This work needs to be extended to include non-linear thermal gradients because the energy equation shows that a linear thermal gradient is a very special case.

Preliminary tests at 90°C show that the compressibility coefficients are highly influenced by temperature. This work needs to be extended into the temperature range of 200°C because many of the overpressured zones are at depths where this is the temperature. This work also needs to be extended to other types of sediments and the measured compressibility coefficients need to be correlated with the Atterberg limits of the sediment.

The variation in depth of a sediment with hydrostatic pore pressure and constant temperature can be described by a power series function of porosity ratio. This work also needs to be extended to include the effect of temperature so as to give a better picture of a normally consolidated formation.

The thermal conductivity of compressed sediment is anisotropic and the horizontal conductivity is greater than the vertical conductivity. The conductivity increases as the porosity ratio decreases.

The permeability of the compressed sediment has been shown to decrease many orders of magnitude faster than the porosity ratio decreases. This strangulation process may cause high pore pressure to develop.

It is important to extend this work to include hydrofracture, because when drilling a well the bore hole pressure at any depth should in general be equal to or greater than the formation pore pressure and less than the pressure that would cause hydrofracture. This applies to all depths not protected by casing. A natural hydrofracture is also thought to limit pore pressures that might develop naturally. Even though there may be several ways hydrofracture can occur each is believed to involve the lateral earth stress at rest, K_0 . For this reason the work needs to be extended to measure K_0 as the sediment is compressed, unloaded, and recompressed.

Finally, it is most important to extend the work to find solutions of the derived governing differential equations for porosity ratio and temperature as a function of depth and time for different boundary conditions. It may be that some generalized iterative technique can be used to solve the equations if analytic methods fail. As a last resort it will probably be possible to get numerical solutions by combining the finite element and finite difference technique. The solution to the equations will show whether overpressures can be generated by thermomechanical processes alone and if steady state pore pressure in excess of hydrostatic pressure can exist.

REFERENCES

1. American Society for Testing Materials, "Density of Plastics by the Density-Gradient Technique," D1505-68, Part 35, ASTM Standards-Plastics, Philadelphia, Pa., 1974.
2. American Society for Testing Materials, "Liquid Limit of Soils D-423-61T and Plastic Limit and Plasticity Index of Soils D-424-59," Part 4, ASTM Standards, Philadelphia, Pa., 1961.
3. Ames, William F., Nonlinear Partial Differential Equations, Academic Press, New York, 1965.
4. Barker, C., "Aquathermal Pressuring: Role of Temperature," Bulletin of American Association of Petroleum Geologists, Vol. 56, No. 10, October, 1972, pp. 2069-2071.
5. Baroid Division, NL Industries, Inc., "Density Gradient Kit Instructions," P. O. Box 1675, Houston, Texas 77001, 1973.
6. Bebout, D. G., Loucks, R. G., and Gregory, A. P., Frio Sandstone Reservoirs in the Deep Subsurface Along the Texas Gulf Coast, Report No. 91, Bureau of Economic Geology, The University of Texas at Austin, Austin, Texas, 1978.
7. Bennett, R. H., Bryant, W. R., Keller, G. H., "Clay Fabric and Geotechnical Properties of Selected Submarine Sediment Cores from Mississippi Delta," NOAA Professional Paper 9, U. S. Department of Commerce, Rockville, Md., 1977.
8. Bennett, R. H., "Piezometer Data and Instrumentation of 1975," Presented at the workshop on Pore Pressures in Submarine Sediments, February 15-16, 1979, NOAA Atlantic Oceanographic and Meteorological Laboratories, 15 Rickenbacker Causeway, Miami, Florida, 33149.
9. Bullard, Sir Edward, "The Flow of Heat Through the Floor of the Atlantic Ocean," Proceedings, Royal Society of London, Series A, No. 222, Feb.-Mar., 1954, pp. 408-429.
10. Carslaw, H. S., and Jaeger, J. C., Conduction of Heat in Solids, Oxford University Press, New York, 1959.
11. Draper and Smith, Applied Regression Analysis, John Wiley, New York, 1966.
12. Eringen, A. C., Mechanics of Continua, John Wiley and Sons, New York, 1967.
13. Fertl, Walter H., Abnormal Formation Pressure, Elsevier, New York, 1976.

14. Fertl, W. H. and Timko, D. J., "How Downhole Temperatures, Pressures Affect Drilling," Part 1, June 1972,
Part 2, (Detecting and Evaluating Formation Pressures) July 1972,
Part 3, (Overpressure Detection from Wireline Methods) August 1972,
Part 4, (Pitfalls in Overpressure Prediction) September 1972,
Part 5, (Predicting Hydrocarbon Environments with Wireline Data) October, 1972,
Part 6, (Correlating Geopressure Gradients with Hydrocarbon Accumulations) November 1972,
Part 7, (The Shale Resistivity Ratio - A Valuable Tool for Making Economic Drilling Decisions) December 1972,
Part 8, (Needless Spending of Drilling and Exploration Money can be Predicted - and Prevented) January 1973,
Part 9, (Novel Ways to Detect Abnormal Pressure) February 1973,
Part 10, (Miscellaneous Ways to Detect Abnormal Pressure) March 1973, World Oil.
15. Fine, R. A., Wang, D. P., and Millero, F. J., "The Equation of State of Seawater," Journal of Marine Research, Vol. 32, No. 3, 1974, pp. 433-456.
16. Gibbs, K. J., X-ray Deffraction Mounts: In Procedures in Sedimentary Petrology, (Ed. by Carver, R. E.) Wiley-Interscience, New York, 1971, pp. 531-559.
17. Hermes, H., "On the Initial Value Problem for the Quasilinear Parabolic Equation," Nonlinear Problems, R. E. Langer, ed., University of Wisconsin Press, Madison, Wisconsin, 1963.
18. Howard, G. C., and Fast, C. R., Hydraulic Fracturing, SPE-AIME Monograph 2, New York, 1970.
19. Kersten, M. S., Final Report Laboratory Research for the Determination of the Thermal Properties of Soils, Engineering Experiment Station, University of Minnesota, Minneapolis, Minn., 1949.
20. Lambe, T. William, and Whitman, Robert V., Soil Mechanics, Wiley, New York, 1969.
21. Lee, W. H. K., and McDonald, G. J. F., "The Global Variation in Heat Flow," Journal of Geophysical Research, No. 68, 1963, pp. 6481-6492.
22. Lewis, C. R., and Rose, S. C., "A Theory Relating High Temperature and Overpressures," Journal of Petroleum Technology, Vol. 22, January 1970, pp. 11-16.
23. Moses, P. L., "Geothermal Gradients," Drilling and Production Practice, 1961.
24. Muskat, M., Physical Principles of Oil Production, McGraw-Hill, New York, 1949.

25. Offshore Rig Data Services, "Offshore Mobile Drilling Rig Accidents 1955 to August 1977," Research and Consulting Division, Houston, 1977.
26. Penner, E., "Anisotropic Thermal Conductivity in Clay Sediments," Proceedings, International Clay Conference, Vol. 1, 1963, pp. 365-376.
27. Powley, Dave, Personal Communication, Amoco Oil Co., Sr. Research Engineer, Amoco Research Laboratory, Tulsa, Oklahoma, 1979.
28. Ratcliffe, E. H., "The Thermal Conductivity of Ocean Sediments," Journal of Geophysical Research, Vol. 65, No. 5, May 1960, pp. 1535-1540.
29. Rogers, Les, "Shale-Density Log Helps Detect Overpressure," The Oil and Gas Journal, September 12, 1968.
30. Skempton, A. W., "Effective Stress in Soils, Concrete and Rocks," out of Pore Pressure and Suction in Soils, Butterworths, London, 1961.
31. Skempton, A. W., "Notes on the Compressibility of Clay," Quarterly Journal of Geology Society of London, Vol. C, London, 1943.
32. Thompson, L. J., "Mechanics Problems and Material Properties," out of Deep-Sea Sediments, Inderbitzen, A. L., ed., Plenum Press, New York, 1974.
33. Thompson, L. J., Robert H. Chen, and William R. Bryant, "Overpressured Marine Sediments," Final Report Phase I, Texas A&M Research Foundation, Project No. 3249, College Station, Texas, January 1977.
34. Truesdell, C., Rational Thermodynamics, McGraw-Hill, New York, 1969.
35. Von Herzon, R., and Maxwell, A. E., "The Measurement of Thermal Conductivity of Deep-Sea Sediments by a Needle-Probe Method," Journal of Geophysical Research, Vol. 64, No. 10, October 1969, pp. 1557-1563.